

ADSORPTION OF WATER ON STANNIC OXIDE

By

JAMES K. SULLIVAN

Bachelor of Science  
Canisius College  
Buffalo, New York  
1965

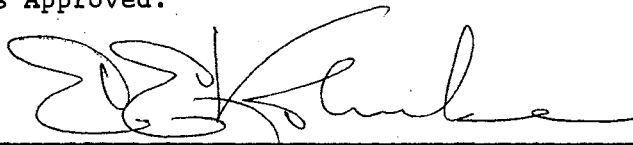
Master of Science  
St. Louis University  
St. Louis, Missouri  
1967

Submitted to the Faculty of the Graduate College  
of the Oklahoma State Univeristy  
in partial fulfillment of the requirements  
for the Degree of  
DOCTOR OF PHILOSOPHY  
May, 1972

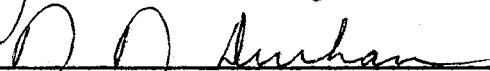
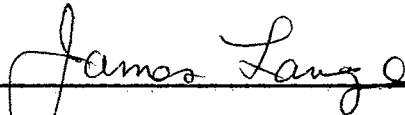
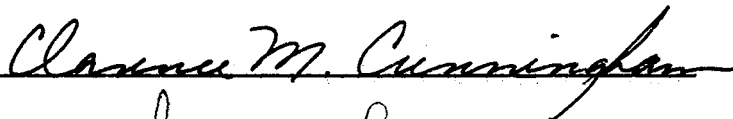
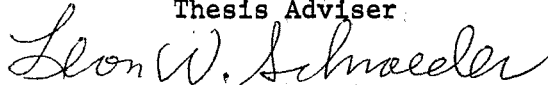
AUG 16 1973

ADSORPTION OF WATER ON STANNIC OXIDE

Thesis Approved:



Thesis Adviser



Dean of the Graduate College

## ACKNOWLEDGMENTS

The author wishes to express his gratitude to Dr. E. E. Kohnke for his supervision and guidance during the course of this study and to the National Aeronautics and Space Administration for support in the form of a traineeship. He is also indebted to the entire faculty and staff of the Physics Department, without whose help and cooperation this study would not have been possible. The author wishes to express his appreciation to fellow members of the research group for their suggestions and stimulating discussion. And finally he wishes to express his gratitude to his wife, Pat, for her assistance and support during this investigation.

## TABLE OF CONTENTS

Chapter	Page
I. BACKGROUND AND THEORY . . . . .	1
A. Conductivity as a Function of Adion Number . . . . .	2
B. Equilibrium Adsorption . . . . .	7
C. Adsorption Kinetics . . . . .	11
D. Desorption Kinetics . . . . .	13
II. EXPERIMENTAL . . . . .	18
A. Equipment . . . . .	18
1. R-Probe . . . . .	18
2. F-Probe . . . . .	20
B. Experiments . . . . .	27
1. Equilibrium . . . . .	27
2. Adsorption Kinetics . . . . .	28
3. Flash Desorption . . . . .	28
C. Samples and Preparation . . . . .	30
III. RESULTS AND CONCLUSIONS . . . . .	33
A. High Temperature Water Adsorption . . . . .	33
1. Adsorption Kinetics . . . . .	37
2. Flash Desorption . . . . .	40
B. Low Temperature Adsorption . . . . .	53
1. Adsorption Kinetics . . . . .	56
C. Suggestions for Further Study . . . . .	64
D. Conclusions . . . . .	66
BIBLIOGRAPHY . . . . .	68

LIST OF TABLES

Table	Page
I. Table of Samples. . . . .	32
II. Difference Table. . . . .	49
III. Short Difference Table. . . . .	49

## LIST OF FIGURES

Figure	Page
1. Band Edge . . . . .	3
2. Chemical Potential . . . . .	9
3. R-Probe Sample Holder . . . . .	18
4. R-Probe Spring Loading . . . . .	19
5. R-Probe Electrical Circuit . . . . .	21
6. R-Probe Ambient Control . . . . .	22
7. Sample Holder . . . . .	24
8. Electrical Measurements-Heater System . . . . .	25
9. Sample Holder System . . . . .	26
10. Flash Desorption . . . . .	34
11. Flash Desorption . . . . .	36
12. Adsorption Kinetics R-37 . . . . .	38
13. Adsorption Kinetics R-48 . . . . .	39
14. Flash Desorption R-38A, B. . . . .	41
15. Flash Desorption R-38C to F. . . . .	42
16. R-38A Time . . . . .	43
17. B Functions. . . . .	45
18. R-38 for $L = 0$ . . . . .	46
19. R-38 for $L = 1$ . . . . .	47
20. R-38 for $L = 2$ . . . . .	48
21. R-49 . . . . .	51
22. R-49 for Assumption B. . . . .	52

LIST OF FIGURES (Continued)

Figure	Page
23. Low Temperature Desorption. . . . .	55
24. Equilibrium R-44. . . . .	57
25. Adsorption I. . . . .	58
26. Adsorption II . . . . .	59
27. Adsorption III. . . . .	60
28. Adsorption IV . . . . .	61
29. Adsorption V. . . . .	62
30. Adsorption VI . . . . .	63

## CHAPTER I

### BACKGROUND AND THEORY

Stannic Oxide is a rutile-structure (1,2) broad-band semiconductor (3,4). A band gap around 4 eV has been indicated by optical work (5,6,7). This value agrees with work by Rutledge (8) which established that conductivity above  $T = 1000^{\circ}\text{K}$  is controlled by an intrinsic mechanism. In the course of studying conductivity below that temperature a two-order-of-magnitude peak was observed at  $10^3/T = 1.62$ , which, as of now, appears to be due to water irreversibly bound to the surface (i.e., bound such that decreasing  $p_{\text{H}_2\text{O}}$  did not desorb it).

A model to account for this behavior and guide further experimentation is to be constructed, incorporating ideas from a variety of sources. The first section of this chapter deals with references to water adsorbed on other materials as well as several different views on how adions could influence sample conductivity. These are combined with previous local work on  $\text{O}_2$  adsorbed on  $\text{SnO}_2$  to give a form for sample conductivity as a function of adion concentration.

Using the results of Section A as a basis, Sections B, C, and D derive equations with which to analyze data obtained in three different situations. Each type of experiment is set up to emphasize and examine the adion-solid system from a different viewpoint.

The lack of a final, definitive theory will be evident in the failure of the three postulated pictures to exactly coincide.



Section B uses published ideas on equilibrium processes and the Law of Mass Action to derive an expression giving the difference between the desorption and adsorption activation energies in terms of electrical conductivity measured under equilibrium conditions. Section C shows how conductivity data taken as a function of time after a sudden exposure of the adsorbent to the adsorbate, emphasizes the adsorption rate, and may be expressed in terms of "Elovich" kinetics. In Section D the desorption process is brought into prominence in terms of data taken during a rapid rise in temperature and a way to analyze such data for activation energy is developed.

#### A. Conductivity as a Function of Adion Concentration

The sorption of an adion will affect the conductivity of a solid to the extent it alters the electronic distribution in the solid. Whether the adsorption involves a single step or a complex of chemical and electronic steps, the sorbate will be herein designated a 'donor gas' if the end result is a majority carrier added to some state in the solid, and as an 'acceptor' gas if the majority charge ends up on the adion. The tendency to become a positive or negative adion can be pictured in terms of energies of the various ionization states relative to the fermi level. That is, if the energy of an electron on a neutral member of the sorbate species is much above the fermi level (as level 1 or 2 in Fig. 1) the sorbate will be found as a positive adion, whereas if the level for an electron occupying the negative ion of that species is much below the fermi level (as level 4 or 5 in Fig. 1) the sorbate will show up as a negative adion.

Hauffe (9) treats the effect of  $O_2$  on n-type oxides, which is an

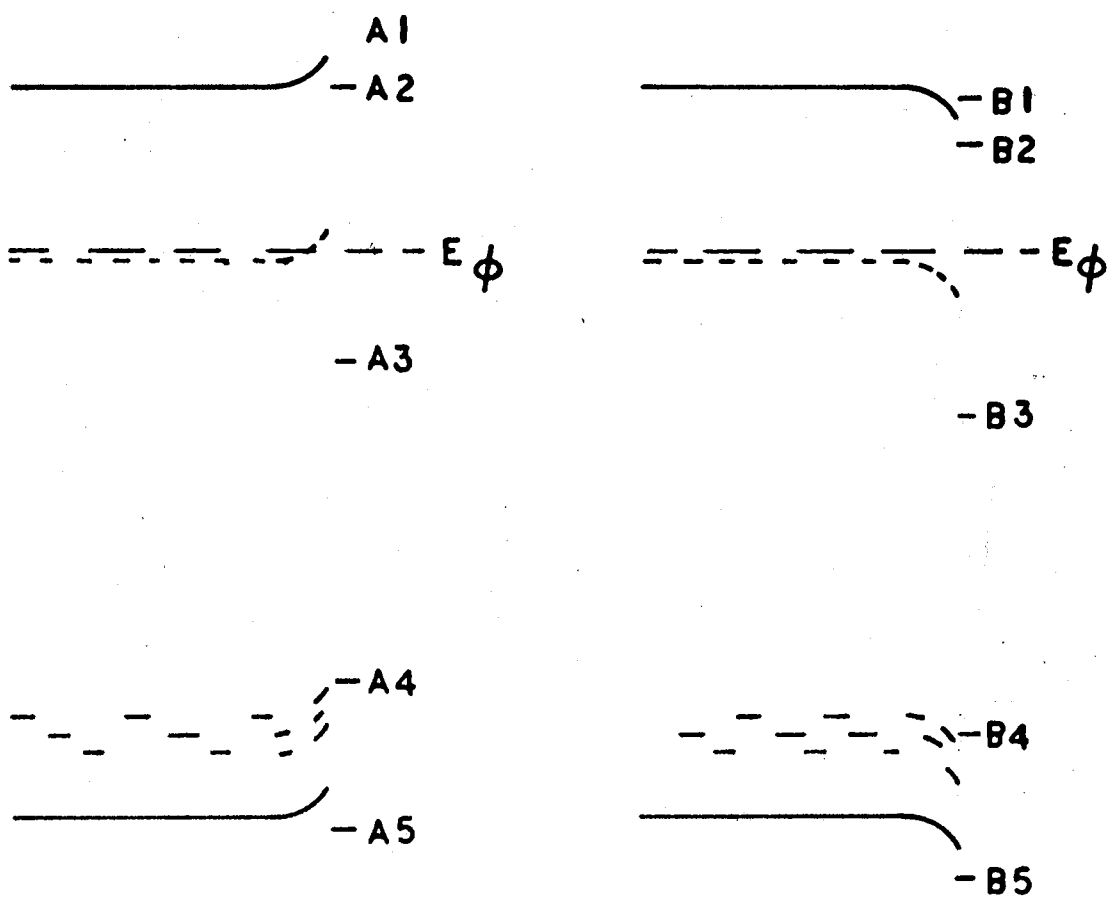


Figure 1. Band Edge

acceptor gas as the term is defined above. He calculates the thickness of a layer that would be totally depleted of majority carriers by the adsorption if the rest of the cross-sectional area of the sample retained the original carrier density.

Morrison (pg. 289 of (10)) analyses the work of others on  $O_2$  adsorbed on ZnO, by "assuming that desorption alone accounts for the conductivity rise." This would seem equal to an assumption that in the bulk ZnO samples, there is no donor level with an energy comparable to the activation energy governing desorption. The temperature dependence of the conductivity would again be dominated by adion number in the case of a donor gas whose level is far enough from the fermi level to be fully ionized (e.g., level a-1 in Fig. 1).

Matthews (11) treated the case of  $O_2$  on  $SnO_2$ . He assumed the electron redistribution represented the effect of adding the adion number to an already sizable number of bulk acceptor centers. In this picture the conductivity before, during and after adsorption is controlled by the same mechanism, with the adion number entering only the pre-exponential coefficient of the electron density expression derived from the partially-compensated semiconductor model (12) in which

$$n \ll N_a \quad (1)$$

is assumed, with the result that

$$n = (N_c/N_a)(N_d - N_a) \exp(-E_E/kT) \quad (2)$$

where  $n$  is the density of conduction electrons,  $N_c$  is the conduction density of states,  $N_d$  is density of donor states at an energy  $E_E$  below the conduction band, and  $N_a$  is the density of acceptors, given as the sum

$$N_a = N_a^* \pm s N \quad (3)$$

with the + for an acceptor gas, the - for a donor gas,  $N_a^*$  the density of all acceptors not affected by the surface reaction, and  $s$  the geometrical factor relating the active surface population,  $N$ , to an effective bulk density.

Substituting Eq. (3) into Eq. (2) using the minus sign for a donor adion leaves

$$n = N_c \left[ \frac{N_d - N_a^* + s N}{N_a^* - s N} \right] \exp(-E_E/kT) \quad (4)$$

Matthews [11] pointed out approximations with which Eq. (4) may be simplified. The basis of these is the relation

$$s N < N_a^* < N_d \quad (5)$$

which is the condition for remaining within the limits of the partially compensated model. The model is exceeded to one extreme if (before the adsorbate is present, when  $N = 0$ )  $N_a^*$  were to outweigh  $N_d$  and bring about total compensation. On the other hand, if (say, during adsorption)  $sN$  passes  $N_a^*$  then all compensators are satiated and the model must be changed.

Within the limits set by Eq. (5) there is much latitude. If one assumes that  $N_a^*$  is small, then, from  $N = 0$  on up one can say

$$N_a \ll N_d \quad (5A)$$

which changes Eq. (4) into

$$n = [N_c N_d / (N_a^* - s N)] \exp(-E_E/kT) \quad (4A)$$

On the other hand, if  $N_a^*$  is assumed to be near its other limit and is of comparable size to  $N_d$ , then the difference  $N_d - N_a^*$  is small. The simultaneous assumption that the adsorbate population is very small compared to  $N_a^*$  allows one to ignore the variable in the denominator of Eq. (4) in favor of its influence on the smaller numerator. Assuming

$$N_d - N_a^* < N_a^* \quad (5B)$$

and

$$N_a^* \gg s N \quad (5B)$$

one may approximate Eq. (4) as

$$n = (N_c/N_a^*) (N_d - N_a^* + s N) \exp(-E_E/kT) \quad (4B)$$

Some references (9, 10, 13) to water adsorption on other materials indicate that  $H_2O^+$  is the adion to expect. Since  $SnO_2$  is n-type this will be a donor gas, and the sign in Eq. (3) is a minus sign.

Unless samples are specially treated, adsorption will occur on a surface already containing  $O_2^-$  ions. The electrons donated by the  $H_2O^+$  adions could simply go to replace electrons used to fill acceptor states with the number of  $O_2^-$  being contained in  $N_a^*$ . Alternately there is the idea of Bliel and Albers (13) in which the  $H_2O$  adsorbed bonds to an  $O_2^-$  by some 'hydrogen bonding' releasing an electron. But this is mathematically equivalent to the first idea since  $N_a^*$ , containing the number of  $O_2^-$  along with the bulk acceptor number, is again reduced by the num-

ber of new adions.

A single-species adsorption of  $\text{H}_2\text{O}^+$ , on a surface from which  $\text{O}_2$  had been desorbed by special treatment, could also fit Eqs. (2) and (3), so long as the number of bulk acceptors minus the number of adions was large enough to satisfy Eq. (1).

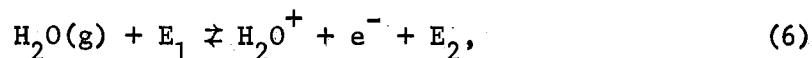
That such a condition is satisfied may be more than a circumstance. It is possible that the number of adions the surface can hold is controlled in some way by the number of bulk acceptors,  $N_a^*$ . For instance, if the adion level were near  $b-2$  in Fig. 1, then conduction electrons could desorb those ions without having to cross a potential barrier. But that desorption rate might remain small enough to be balanced by adsorption if the number of conduction electrons remains small. But if a point were reached where condition (1) were no longer fulfilled, then each electron donated by an adion would remain in the conduction band (instead of one out of a hundred or less as when Eq. (1) still holds). Thus, the critical value of  $N$  for (1) may also be the critical value for the adsorption process.

The above is offered not as a definitive or even analytic theory, but only as one more physical possibility which the equations may represent.

#### B. Equilibrium Adsorption

Taking data at constant pressure-temperature points emphasizes the equilibrium of two processes, adsorption and desorption. Each process may be compounded of several steps (14), in each of which a separate potential barrier is crossed. The observable rate of a multistep process is controlled by the rate of the slowest step. Throughout the following

treatment expressions will be written as if only single steps were involved, but each rate equation may as well represent the limiting step of a series. The equilibrium of two simple rates may be viewed in terms of a potential diagram like Fig. 2. The rate of leaving a state, say state 2, is proportional to the concentration(s) of the component(s) times the Boltzmann exponential. For a simple process expressed as



where  $E_1$  and  $E_2$  are energies as in Fig. 2, the rates of adsorption,  $r_a$ , and desorption,  $r_d$ , are given as

$$r_a = c_a p_{\text{H}_2\text{O}} \exp(-E_1/kT) \quad (7)$$

and

$$r_d = c_d^n N_{\text{H}_2\text{O}^+} \exp(-E_2/kT) \quad (8)$$

where  $c_a$  and  $c_d$  are proportionately constants,  $N_{\text{H}_2\text{O}^+}$  is the concentration of water adions,  $p_{\text{H}_2\text{O}}$  is the partial pressure of water and  $n$  is the concentration of conduction electrons. This assumes the rate limiting step for adsorption is the one from adion plus associated electron (Making a neutral molecule) to adion held at the surface plus electron in the conduction band. When Eq. (1) holds the fermi level is controlled by  $N_a$  and so most of the electrons replace ones taken from  $N_d$  by acceptor states, but they will do so by subsequent steps assumed much faster than (6).

Equating  $r_a$  and  $r_d$  and defining

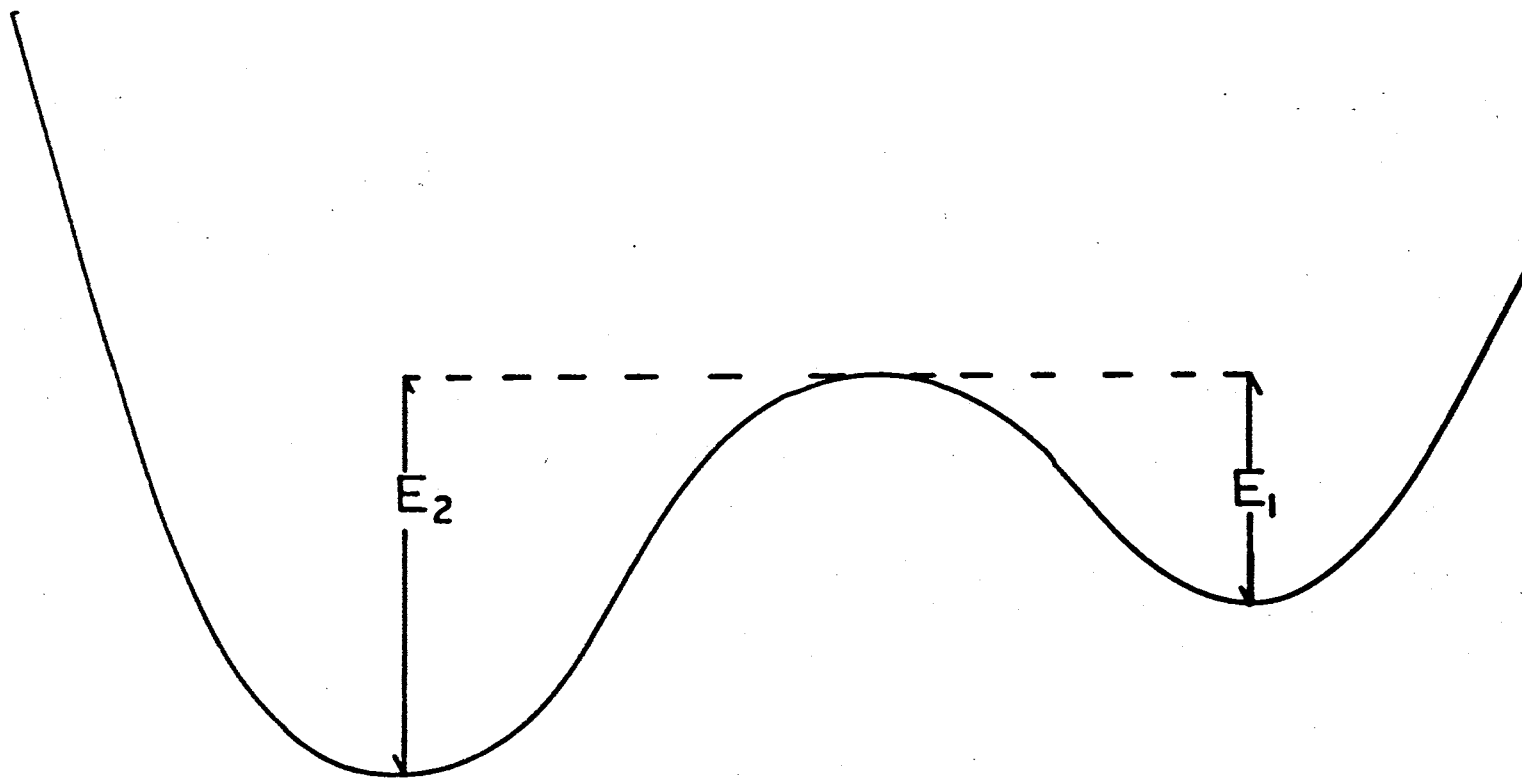


Figure 2. Chemical Potential



$$\Delta E \equiv E_1 - E_2, \quad (9)$$

yields

$$n \frac{N_{H_2O^+}}{P_{H_2O}} = C \exp (\Delta E/kT), \quad (10)$$

where the constants have been combined into C. This is the same mass action equation which Kroger and Vink (15) derived from a chemical potential view of equilibrium.  $\Delta E$  is positive since the equilibrium is observed to shift to the gas phase as T goes up.

The final expression predicting the data is obtained by solving (10) for  $N_{H_2O^+}$  and using it for the N in Eq. (5). That is

$$n = \frac{N_c N_d \exp (-E_E/kT)}{N_a^* - s c P_{H_2O} n^{-1} \exp (\Delta E/kT)}, \quad (11)$$

which may be solved for n as

$$n = (sc/N_a^*) P_{H_2O} \exp (\Delta E/kT) + (N_c N_d/N_a^*) \exp (-E_E/kT). \quad (12)$$

This predicts two zones: one at high temperature where the sample ignores any moisture and the second at lower temperature where the current will decrease with increasing temperature, with a semi-log slope given by  $\Delta E$ .

Morrison (10) in his work on ZnO, describes a third region where  $kT$  is so low that one or both rates are too slow to give a measurable effect during an experiment. If such a region is found for  $H_2O$  on  $SnO_2$ , n and conductivity would depend on past history as well as the variables of

Eq. (11).

### C. Adsorption Kinetics

The two rates,  $r_a$  and  $r_d$ , may be experimentally separated by examining nonequilibrium, time-varying situations. One experimental way to focus on  $r_a$  is with  $p_{H_2O}$  given as

$$p_{H_2O} = \begin{cases} p^0, & t < 0 \\ p', & t \geq 0 \end{cases} \quad (13)$$

where  $p'$  is a constant which may be varied from run to run. This sudden increase in sorbate pressure allows

$$r_d \ll r_a$$

for a measurable time.

Low (16) reviews a variety of experiments in which chemisorption occurs. Among them he finds one form of adsorption rate so consistent that he uses it as an organizing basis for his review. This is mathematically described by the Elovich equation

$$dN/dt = a \exp(\alpha N) \quad (14)$$

which integrates to

$$N(t) \propto \ln(t + k). \quad (15)$$

After briefly reviewing a bewildering array of models he says (see pg. 307 of (16)) "the more general models....suffer because their flexibility seems to preclude quantitativity. Conversely, the more quantitative

approaches seem at present to be imbued with too much rigor, and cannot account for the complex behavior found experimentally."

One of the latter is the band-bending model (10, 17). For the case defined in Section I as an acceptor gas (e.g., oxygen on an n-type solid) this model equates the concentration-dependent activation energy of the Elovich equation with the energy barrier caused by the space charge layer. This assumed picture would be like Fig. 1A for an n-type sample with electrons crossing the barrier out of the conduction band as the rate limiting step for adsorption. One of the problems of this model is that it places  $n$ , the conduction carrier density, in the pre-exponential coefficient of (14) or (7) making its integration more difficult. Medved (17) claims that this will still give a good fit up to 10% change in  $n$ . Data taken for  $O_2$  on  $SnO_2$  (11, 18-21) fit (15) for much larger changes in  $n$ . But  $n$  need not be in the coefficient at all if one postulates some step to replace electron transfer as the rate limiting step. As yet, however, no other explanation for the coverage-dependent energy has offered such a clear, visually analytic picture as has the band-bending concept.

The observation of Elovich adsorption kinetics for a donor gas on an n-type material would provide a further indication that the source of such behavior should be sought in other directions. Although it has been suggested that adsorption of a donor gas could still be controlled by band-bending if it were dependent on the capture of a minority carrier, such a dependence would imply an adion energy level far below the fermi level (as b-4 in Fig. 1). A positive ion so far below the fermi level would not be stable.

Assuming there is some, as yet, unspecified rate limiting step,

whose mechanism does include a coverage-dependent energy, Eq. (15) may be substituted into Eq. (5) to yield

$$i^{-1} = \frac{C_1 - C_2 \ln(t+k)}{C_3} \quad (16A)$$

with  $C_1$ , thru  $C_3$  constants dependent on parameters of the material and initial conditions. But substituting Eq. (15) into Eq. (4B) gives

$$i = C_4 + C_5 \ln(t + K) \quad (16B)$$

#### D. Desorption Kinetics

To bring the desorption process into focus, conditions must be such that  $r_a$  is relatively small and  $r_d$  is large. Reference to Eqs. (7) and (8) shows the parameters involved.  $r_a$  may be made small by keeping  $p_{H_2O}$  small. In the case of equilibrium between  $r_a$  and  $r_d$ , a small  $p_{H_2O}$  will give only a small  $N_{H_2O+}$ . But if  $T_o$ , the starting point of a temperature rise, can be experimentally made low enough that

$$E_2 \gg kT_o \quad (17)$$

then  $p_{H_2O}$  can be lowered without emptying  $N_{H_2O+}$ . Then  $r_d$  may be made measurable by subjecting the sample to a rapid heating program.

Such experiments have been done by Redhead (22) and by Carter (23, 24) on systems such as  $H_2$  on W. These papers provide formulae to obtain the instantaneous desorption rate from the various vacuum system parameters measured during a linear or inverse temperature increase of from  $1^\circ K/sec$  to  $1000^\circ K/sec$ . In each paper the rate equation is assumed, without physical argument to be

$$dN/dt = v N^{\ell} \exp (-E_d/kT) \quad (18)$$

where  $N$  is the surface population,  $\ell$  is the order of kinetics,  $E_d$  is the desorption activation energy and  $v$  is a constant.

Equation (18) may be separated and integrated to

$$\int_{N_0}^N N^{-\ell} dN = -v \int_0^t \exp (-E_d/kT) dt \quad (19)$$

A number of solutions for the integral on the right side are offered in the literature (25 thru 31) referred to as "Glow Curve Analysis" because it arose in Thermally Stimulated Luminescence and other similar experiments. In these papers a linear heating rate is assumed. The resulting integral can be approximated in ten or twenty terms of the semi-convergent asymptotic series, as developed by Chen (28). Paterson (30) criticizes this on the basis that, although the error is small it varies wildly, thus distorting any analysis based on curve shape. Shenker and Chen (31) describe the iterative process and arbitrary choice of starting  $E_d$  value used to evaluate the activation energy.

This author has developed a more general solution. This solution allows use of a less restrictive heating curve and transfers the burden of truncation from an abstractly mathematical manipulation to an evaluation of the data's limit of precision. The solution defines

$$X \equiv 1/T. \quad (20)$$

Then repeated integration by parts gives

$$\int_0^t \exp (-E/kT) dt = [B(x,E) \exp (-x E/k) \Big|_{x=1/T_0}^{x=1/T} \quad (21)$$

where

$$B(x,E) \equiv - \sum_{n=1}^{\infty} (k/E)^n d^n t / dx^n \quad (22)$$

Here the data is treated in terms of time as a function of  $x$ . Taking data at equal intervals of  $10^3/T$  facilitates making a difference table and finding (32) the constants for

$$t = \sum_{j=0}^J b_j (10^3 x)^j, \quad (23)$$

to represent the heating curve. The  $J$  value is that order of difference at which the noise swamps the ideal value and randomness appears (33).

Thus  $B(x,E)$  is a polynomial.

The left hand side of (19) becomes

$$\int N^{-\ell} dN = \begin{cases} \frac{N^{1-\ell} - N_0^{1-\ell}}{1-\ell}, & \ell \neq 1 \\ \ln(N/N_0), & \ell = 1 \end{cases} \quad (24)$$

Now the function of data to go on an Arrhenius plot may be found. To eliminate the donor depth, divide expressions of the form of (5) for two currents, leaving

$$i_c / i_A = (N_a^* - s N) / N_a^* \quad (25)$$

when  $i_A$  is the current during the desorbing rise in temperature, and  $i_c$  is the current during a subsequent identical heating program with a fully desorbed starting condition (to be indicated by the reproducibility of  $i_c$  in the absence of adsorbate). Now solving Eq. (25) for  $N(i_c/i_A)$  and using Eqs. (19), (21) and (24) yields the following set of equations.

$$v B(x,E) \exp(-E/kT) = f(\text{data};\ell) \quad (26)$$

with

$$f(\text{data};\ell = 0) = c_0 [i_c/i_A - \delta] \quad (27)$$

$$f(\text{data};\ell = 1) = \ln(1 - i_c/i_A) - \ln(1 - \delta) \quad (28)$$

$$f(\text{data};\ell = 2) = c_2 \frac{(i_c/i_A - \delta)}{1 - i_c/i_A} \quad (29)$$

where

$$\delta \equiv 1 - s N_o/N_a^* = i_c(T_o)/i_A(T_o) \quad (30)$$

is to be measured at the initial temperature  $T_o$ .

Using Eq. (4B) instead of Eq. (25) to find  $i_c/i_A$  gives

$$f_B(\text{data};\ell = 2) = \frac{\frac{\delta}{1-\delta} - \frac{i_c/i_A}{1-i_c/i_A}}{N_d - N_a^*} \quad (29B)$$

## CHAPTER II

### EXPERIMENTAL

#### A. Equipment

Several different sets of equipment were used. Herein each will be explained separately and throughout the thesis each will be referred to by a single letter and the word "Probe."

##### 1. R-Probe

The designation "R-Probe" refers to a device (8) capable of measuring the temperature and conductivity of a sample in a dark, controlled ambient, in the temperature range from room temperature to 1200°C.

The sample is held by spring pressure between two platinum contacts, each of which is joined to one platinum wire and to one platinum -10% rhodium wire. These wires are held separate by two hole, alumina capillaries, which are in turn supported and aligned by a larger alumina tube as shown in Fig. 3. The spring loading of the upper capillary and this support for the other ceramic components is shown in Fig. 4. Where necessary the brass is glued to the ceramic with Torr Seal epoxy. The vacuum seal is accomplished by gluing the ceramic capillary into the stainless steel flange. The lead wires are sealed to the capillary with Torr Seal with the epoxy not touching that which seals to the capillary the flange, thus insuring that the only electrical leakage path is through alumina.



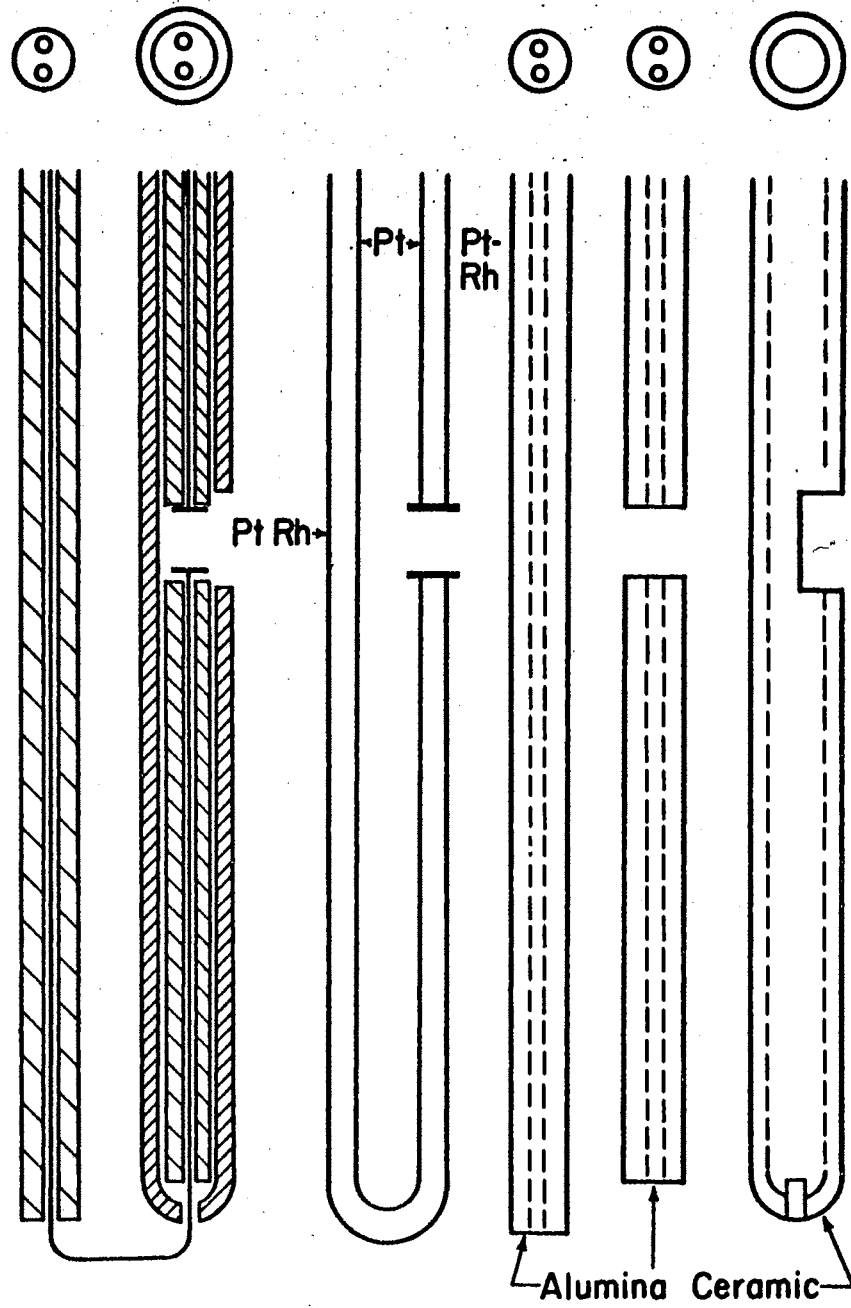


Figure 3. R-Probe Sample Holder (After Rutledge)

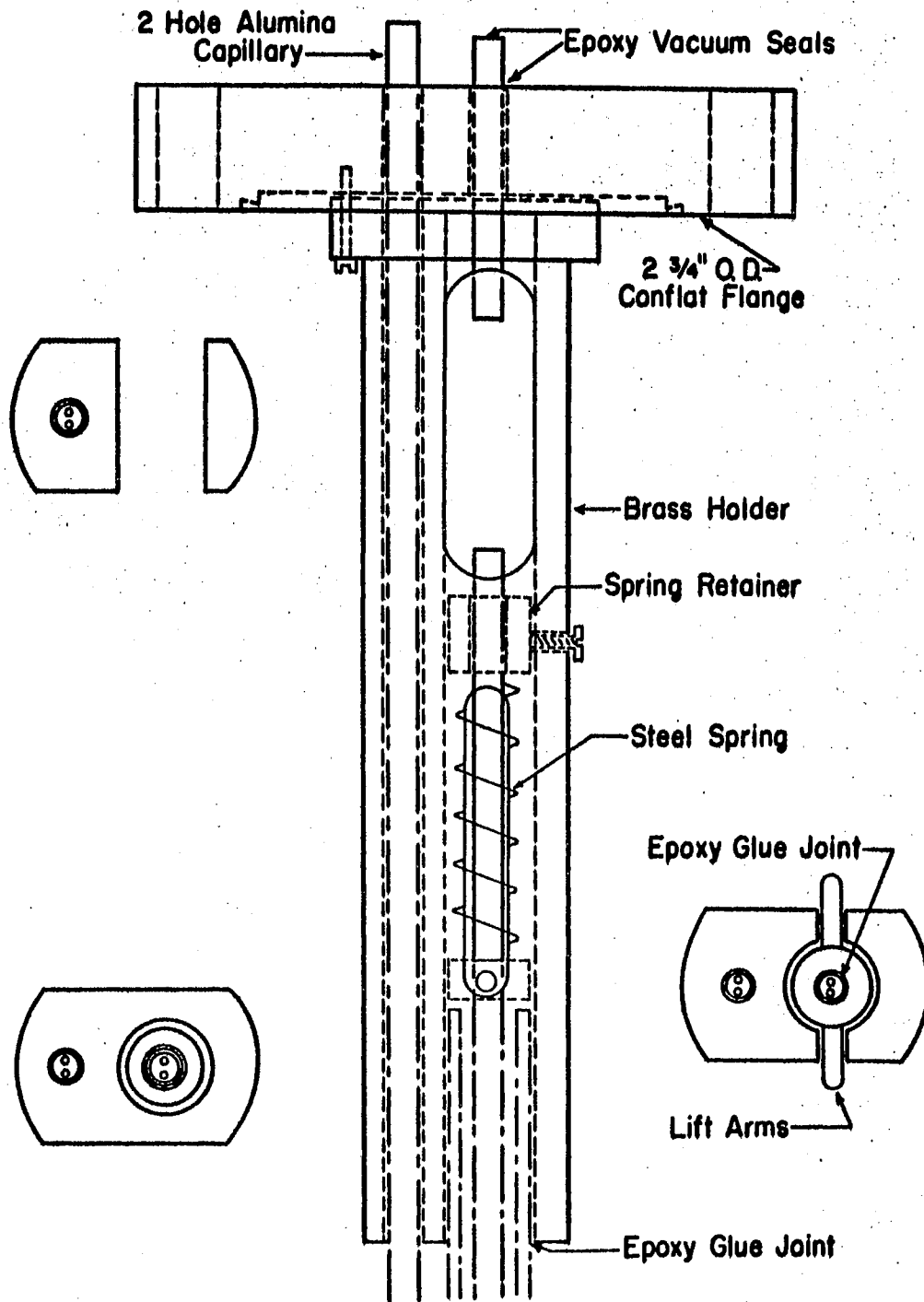


Figure 4. R-Probe Spring Loading (After Rutledge)

The sample current flows through the platinum leads to a floating ground battery (usually around one and a half volts), and then through a Keithley 602 Electrometer, whose reading is recorded on one Sargent model SR strip chart recorder (see Fig. 5).

The thermocouple voltage from the Pt-Pt 10% Rh junction of either end of the sample can be read, in reference to an ice-water temperature junction, on the second SR recorder. When sample resistance is low, the current can become so large that the IR drop in the shared platinum lead is comparable to the thermocouple voltage. Then the sample current must be interrupted to allow a true temperature reading.

Figure 6 shows the ambient control system and the external movable heater. For high temperature an alumina tube was used for the part that projects into the heater. At lower temperatures (below  $1000^{\circ}\text{K}$ ) a stainless steel tube was used since it served at the same time as vacuum chamber and guard against spurious electrical influences.

Pressure readings from  $10^{-4}$  torr to 760 torr were obtained with the Alphatron vacuum gage. Lower pressures could be read on the indicator of the Vacion pump. All seals are Con-Flat 2 3/4" O.D. flanges, except for ceramic-to-metal seals, which are Torr Seal epoxy. The epoxy must be kept below  $100^{\circ}\text{C}$ .

Other options beside vacuum or room air, were obtained by modifications beyond "Gas Inlet" in Fig. 6. Among these were flowing room air through a desiccator, using bottled dry  $\text{N}_2$ , and using  $\text{N}_2$  bubbled through  $\text{H}_2\text{O}$ .

## 2. F-Probe

The designation F-Probe refers to a device capable of measuring the

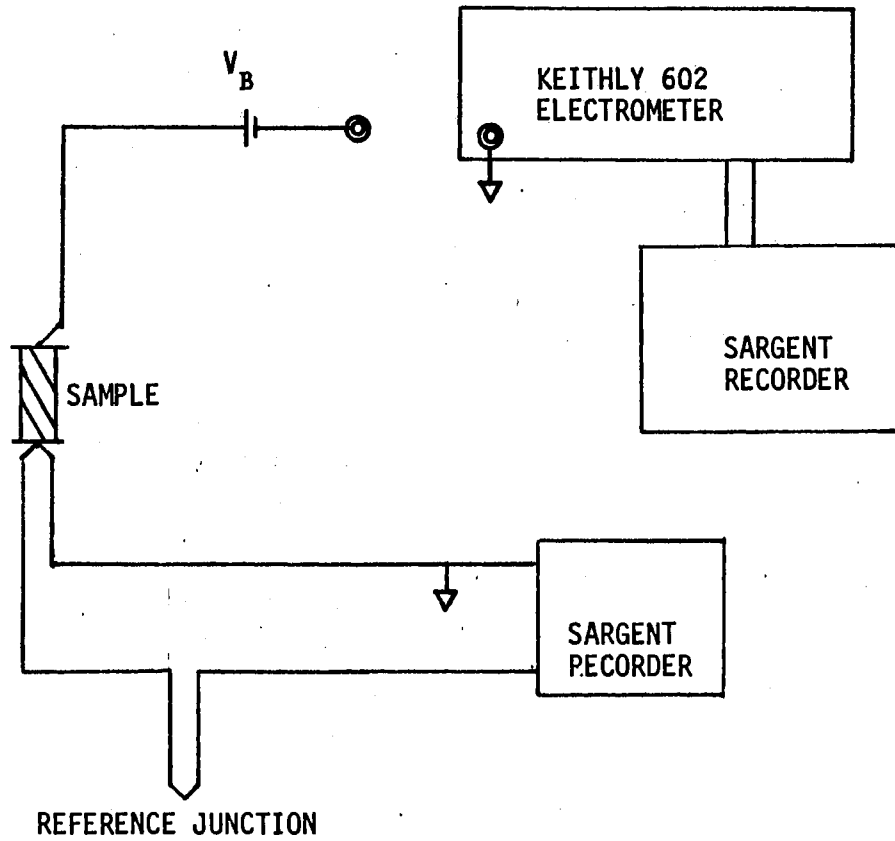


Figure 5. R-Probe Electrical Circuit.

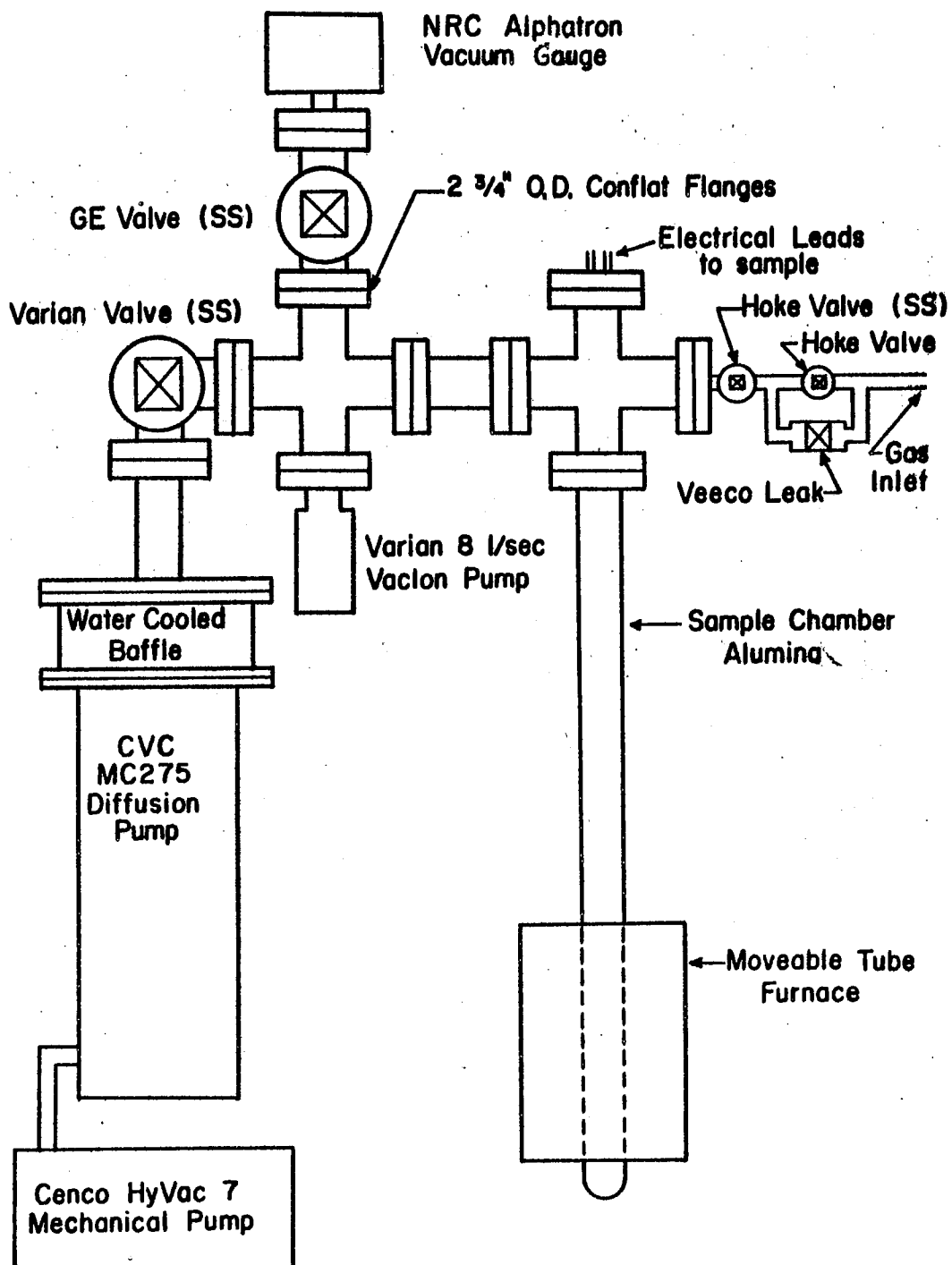


Figure 6. R-Probe Ambient Control (After Rutledge)

temperature and conductivity of a sample from 100°C down to liquid N<sub>2</sub> temperatures, with a controlled ambient, and with the option of illuminating the sample with ultraviolet light.

The sample is held, as shown in Fig. 7 between a fixed platinum contact and a spring loaded copper contact, which is joined to a copper lead and to a Constantan lead. This same figure shows the heater arranged with thermal contact to the copper tube surrounding the sample.

Figure 8 shows the sample current circuit and the heater circuit. The thermocouple voltage is measured on a Sargent model S.R. recorder. The current goes through a one and a half volt floating ground battery and a Keithley 602 Electrometer, which records on a second model SR recorder.

In Fig. 9 can be seen sample current lead. The return path for this circuit is through the outside of the coax leads and through the walls of the cryostat. Resistance from the outside of the BNC connector shown in Fig. 9 to the copper arm of the thermocouple was measured at less than one ohm.

Figure 9 also shows the cooling reservoir, the vacuum chamber and the quartz view port. All joints of the chamber were soldered, and the quartz window was sealed in the port with Apiezon W vacuum wax.

The gas port leads to a three way valve, which can connect the chamber to a fore pump, or allow the inlet of some specified gas (e.g. desiccated air, dry N<sub>2</sub> or N<sub>2</sub> bubbled through H<sub>2</sub>O). Gas pressure was measured on the thermocouple gage, as well as on a mercury monometer placed at the gas inlet beyond the through way valve.

When ultraviolet was used, it was produced by a Hg-light source, which shone directly into the quartz port. No lenses or filter were

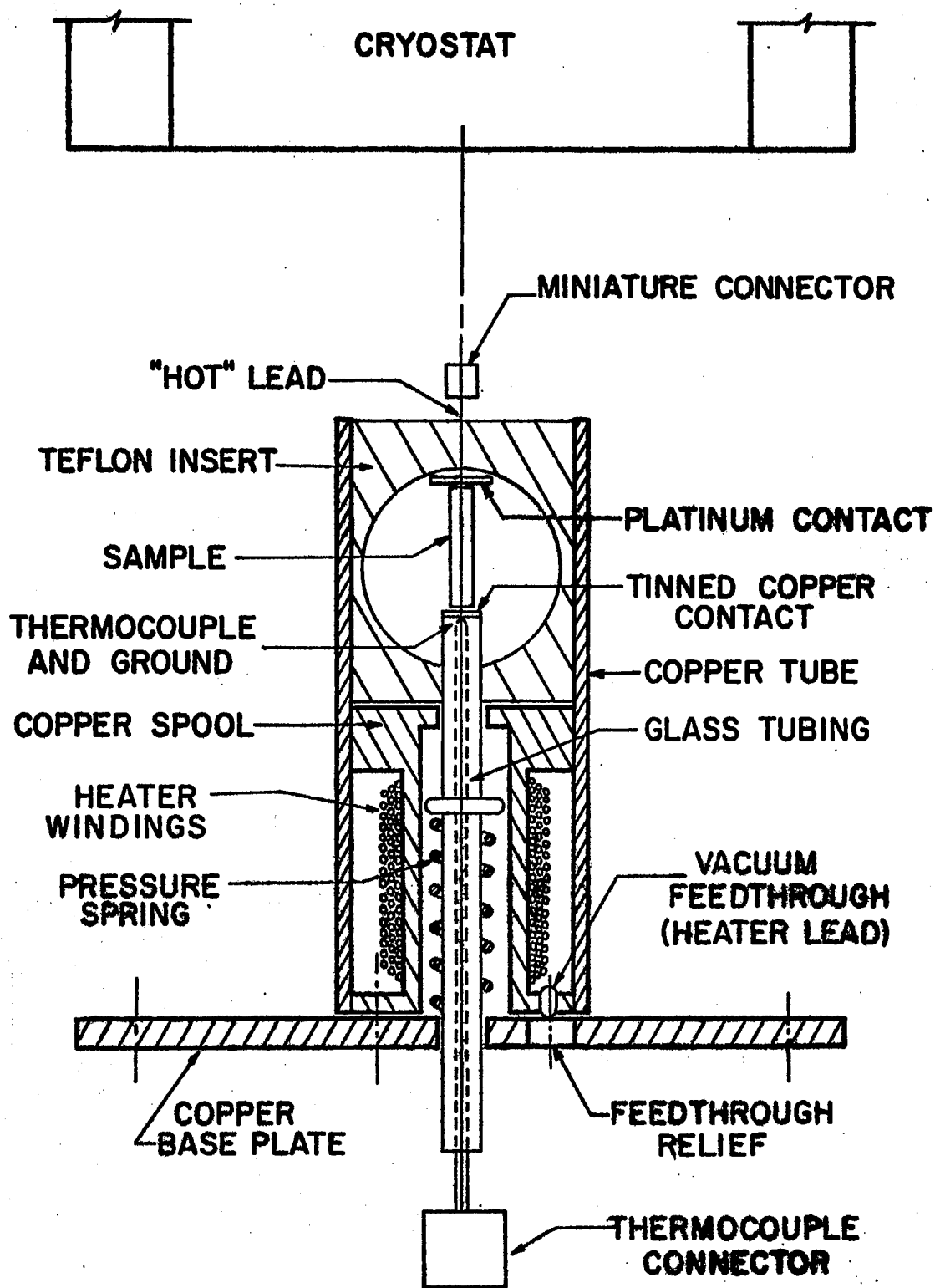


Figure 7. Sample Holder  
(After  
Freeman)

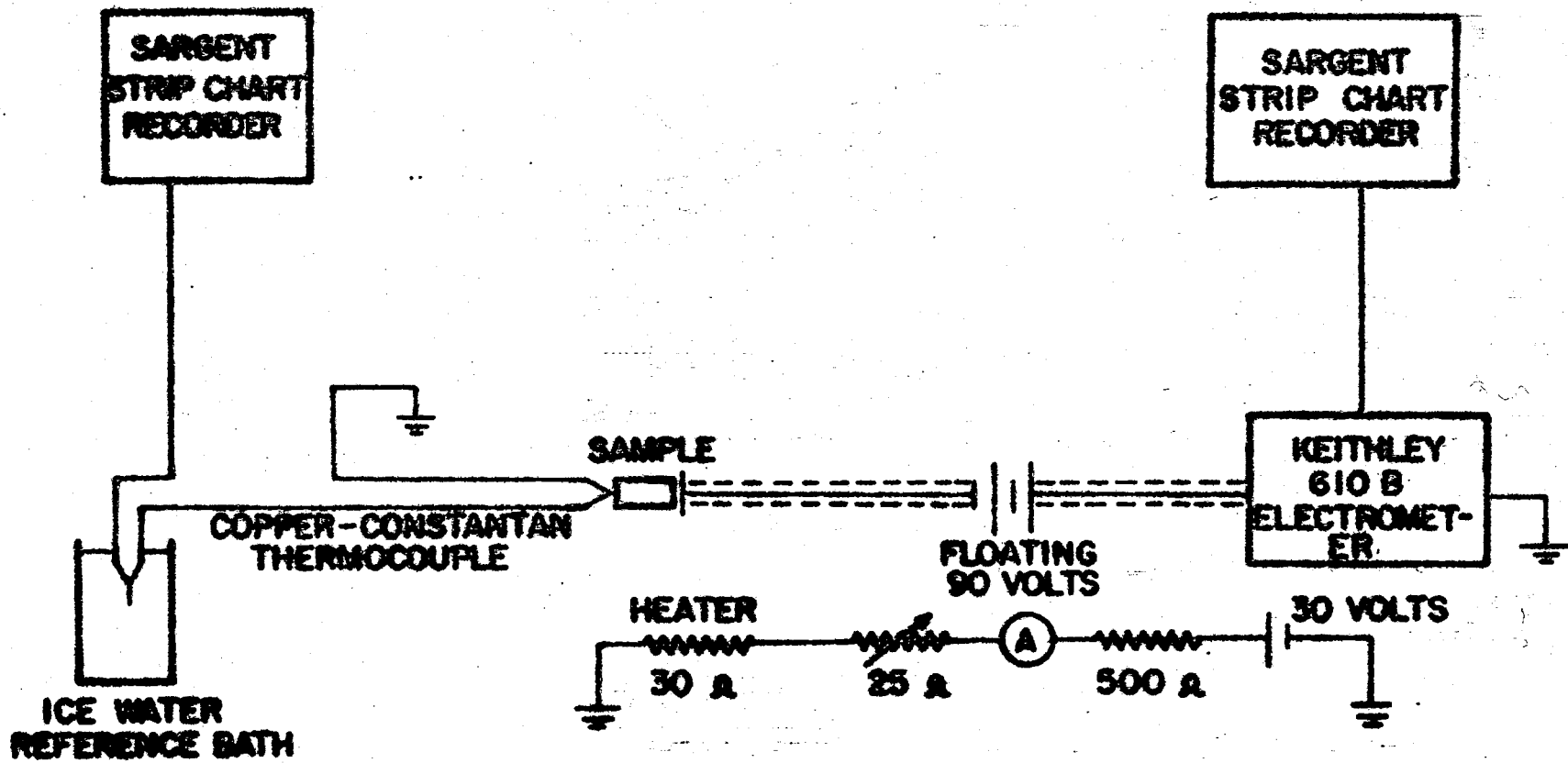


Figure 8. Electrical Measurements-Heater System  
(After Freeman)



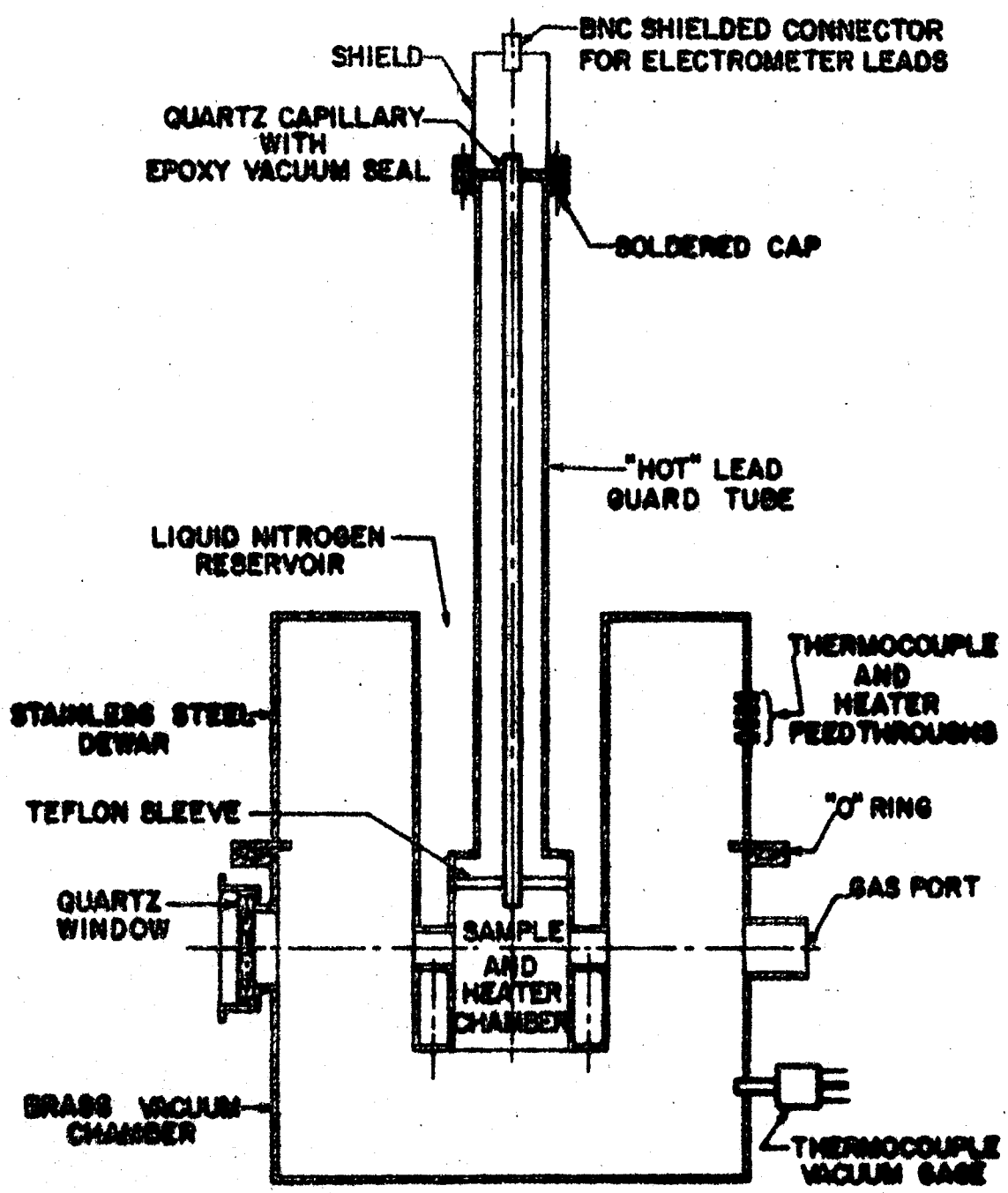


Figure 9. Cryostat Sample Holder System  
(After Freeman)

used.

## B. Experiments

In each of the foregoing setups there are a number of parameters under the control of the experimenter. Consideration of the various ways a single parameter may be changed shows that the combinations which each amount to a different type of experiment are numerous. In the following subsections three of these patterns of parameter handling will be described. These three have been chosen for their significance in terms of the three methods of analysis developed in Chapter I. Other patterns have been tried, and some comment will be included in Chapter III, for those showing a clear significance.

In each of the three the parameter measured was simple current, due to a known, constant voltage. The other parameters are temperature, and its rate of change, and the type and pressure and rate of pressure change of the ambient gas.

### 1. Equilibrium

To fit the assumptions of Section I-B, the rate of change of the temperature as well as of the pressure must be negligible.

Analysis of the Data is straight forward using Eq. (12), with current assumed proportional to  $n$ , yields the prediction that

$$i \propto p_{\text{H}_2\text{O}}, T \text{ constant} \quad (31)$$

$$\log(i) \propto E/kT, p_{\text{H}_2\text{O}}, \text{ constant.} \quad (32)$$

Thus a graph of  $\log(i)$  versus  $10^3/T$  should give a value for  $\Delta E$ .

Experimental Difficulties with this type of experiment seem largely concerned with time. If too long a time is allowed for temperature to equilibrate, minor fluctuations in pressure or composition of ambient will build up. The various compromises made at various points will be indicated in discussing the data in Chapter III.

## 2. Adsorption Kinetics

To fit the assumptions of I-C, temperature should be held constant while the adsorbate is admitted suddenly. When the sorbate is admitted to an evacuated sample chamber, the temperature often changes because the sorbate will conduct heat between the sample and chamber walls. The chamber may be initially filled with some neutral gas (e.g.,  $N_2$ ), but then this must be flushed out by the sorbate.

Analysis of the Data amounts to plotting the current or its inverse as a function of  $\log$  time. The evaluation of the  $t'$  constant as well as of slopes and the dependence of each on temperature and pressure has not been here in approached for lack of a model yielding adequately clear predictions.

## 3. Flash Desorption

Samples for flash desorption must be brought below a  $T_0$  fulfilling Eq. (17).

After adsorption, the sample temperature is lowered until Eq. (17) is true, and the adsorbate is replaced by a neutral gas or vacuum. The heating program used consisted of a single heater power setting. After

the desired maximum temperature was reached, the heater was shut off and the sample allowed to cool. Current and temperature were monitored continuously. A second, and occasionally a third, cycle of temperature were used to provide the " $i_c$ " of Eq. (25). The third cycle provides the proof that the sample was in a fully desorbed state at the start of the second cycle, for only if such were true could the second and third cycles have identical Arrhenius plots.

Data Analysis here consists of two parts. First the  $f(\text{data}; \ell)$ , for a presumed value of  $\ell$ , from Eq. (27 through 29) is plotted on a Arrhenius plot. Then it is modified by  $B(x, E)$ .

Once the  $b_j$  and  $J$  of Eq. (23) are found numerically (see ref. 32 and 33), one needs  $B(x, E)$ . Taking derivatives of Eq. (23), gives

$$\frac{dt^n}{dx^n} = \sum_{j=n}^J b_j 10^{3j} x^{j-n} j!/(j-n)! \quad (33)$$

which goes into Eq. (22) to give

$$B(x, E) = - \sum_{n=1}^J (k/E)^n \sum_{j=n}^J b_j 10^{3j} x^{j-n} j!/(j-n)! \quad (34)$$

Picture the elements to be summed as spread out in an array with  $j$  the column and  $n$  the row. The elements along each diagonal have the same power of  $x$ . Let that be a new dummy index,

$$\ell = j - n \quad (35)$$

Summing over elements of equal  $\ell$  first and then over the values of  $\ell$  yields:

$$B(x, E) = - \sum_{\ell=0}^{J-1} \sum_{j=\ell+1}^J x^{\ell} b_j 10^{3j} (j!/\ell!) (k/E)^{j-\ell} \quad (36A)$$

or

$$B(x, E_1) = - [10^3 k/E] \sum_{\ell=0}^{J-1} (10^3 x)^{\ell} B_{\ell}^i \quad (36B)$$

with

$$B_{\ell}^i = \sum_{j=\ell+1}^J b_j (10^3 k/E_1)^{j-\ell-1} j!/\ell! \quad (37)$$

The first  $(10^3 k/E)$  is lost in the pre-exponential constant.  $E_0$  may be taken as very large, so

$$B_{\ell}^0 \approx (b_{\ell+1}) (\ell+1) \quad (38)$$

can be used in a  $B(x, E_0)$ . For a first approximation this is divided into  $f(\text{data})$ . These divisions can be done graphically, if  $B(x, E_1)$  are graphed on a semilog of the same scale as  $f(\text{data})$ . The resulting plot will yield a value of  $E_1$ . Further such iterations of evaluating  $B(x, E_1)$  and re-evaluating  $E_1$  should proceed until changes in  $E_1$  are small compared to other limits of precision. (A few iterations have suffered throughout this work.)

### C. Samples

The ceramic samples used in this study are identified by the letter "S" followed by a number. The data in Chapter III is labeled in this way and the specifics for each sample are to be found under that number in Table I.

Fabrication of each sample followed the same general pattern. Powdered  $\text{SnO}_2$  along with the dopant, if any, were mixed in an acetone slurry, allowed to dry overnight and then pressed at 10,000 psi. They were again allowed to dry before firing. Firing times indicated in Table I are the time spent at the indicated temperature.

As fired the samples were disks one inch in diameter and about one eighth inch thick. The samples were cut to the size shown in Table I by a carborundum saw. (See ref. 11 for further details.)

Before mounting, samples were washed by the following procedure:

- a) 3 washes in acetone in ultrasonic cleaner
- b) 2 washes in methanol in ultrasonic cleaner
- c) 2 washes in distilled water in ultrasonic cleaner
- d) Boiling for 15 minutes in aqua regia
- e) 1 rinse in distilled water
- f) Boiling for 15 minutes in hydrochloric acid
- g) 4 rinses in distilled water in ultrasonic cleaner
- h) 2 rinses in methanol in ultrasonic cleaner

TABLE I.

TABLE OF SAMPLES

#	Dopant	Edges (mm.)	Firing	
			Time	Temp.
7	.7% wt. ZnO	5.99	4 hr.	1315°C
		2.27		
		1.73		
16	-----	5.34	16 hr.	1245°C
		2.51		
		1.97		
22	.7% wt. ZnO	4.98	4 hr.	1460°C
		2.81		
		1.22		

## CHAPTER III

### RESULTS AND CONCLUSIONS

The adsorption of water on  $\text{SnO}_2$  is observed to comprise at least two distinct ranges or processes. The two are herein labeled "Low temperature" and "High temperature." The low temperature adsorption is observed as an equilibrium process from room temperature to less than  $400^\circ\text{K}$ . The high temperature process appears as water bound irreversibly at room temperature and begins to become reversible after  $10^3/T = 1.7$  or  $1.8$  (i.e., about  $600^\circ\text{K}$ ). The data and results for each are given below as separate sections.

#### A. High Temperature Water Adsorption

The high temperature adsorption was first observed on conductivity data taken at finite rates of temperature change. In the following examples, to facilitate comparison, the data given in the next twelve figures are from the same sample, S-7 (see Table I). Fig. (10) shows a series of curves of log conductivity vs.  $10^3/T$ . On the first branch the arrows indicate heating or cooling. Prior to branch R-29, the sample received no heat treatment since fabrication. The maximum on the heating branch of R-29 failed to reproduce on cooling. It appeared much smaller the next time (R-30) heated and was smaller still the third time (R-31). Between R-31 and R-32 the sample was exposed to laboratory air in the light tight R-Probe, for six days. Note that the maximum con-



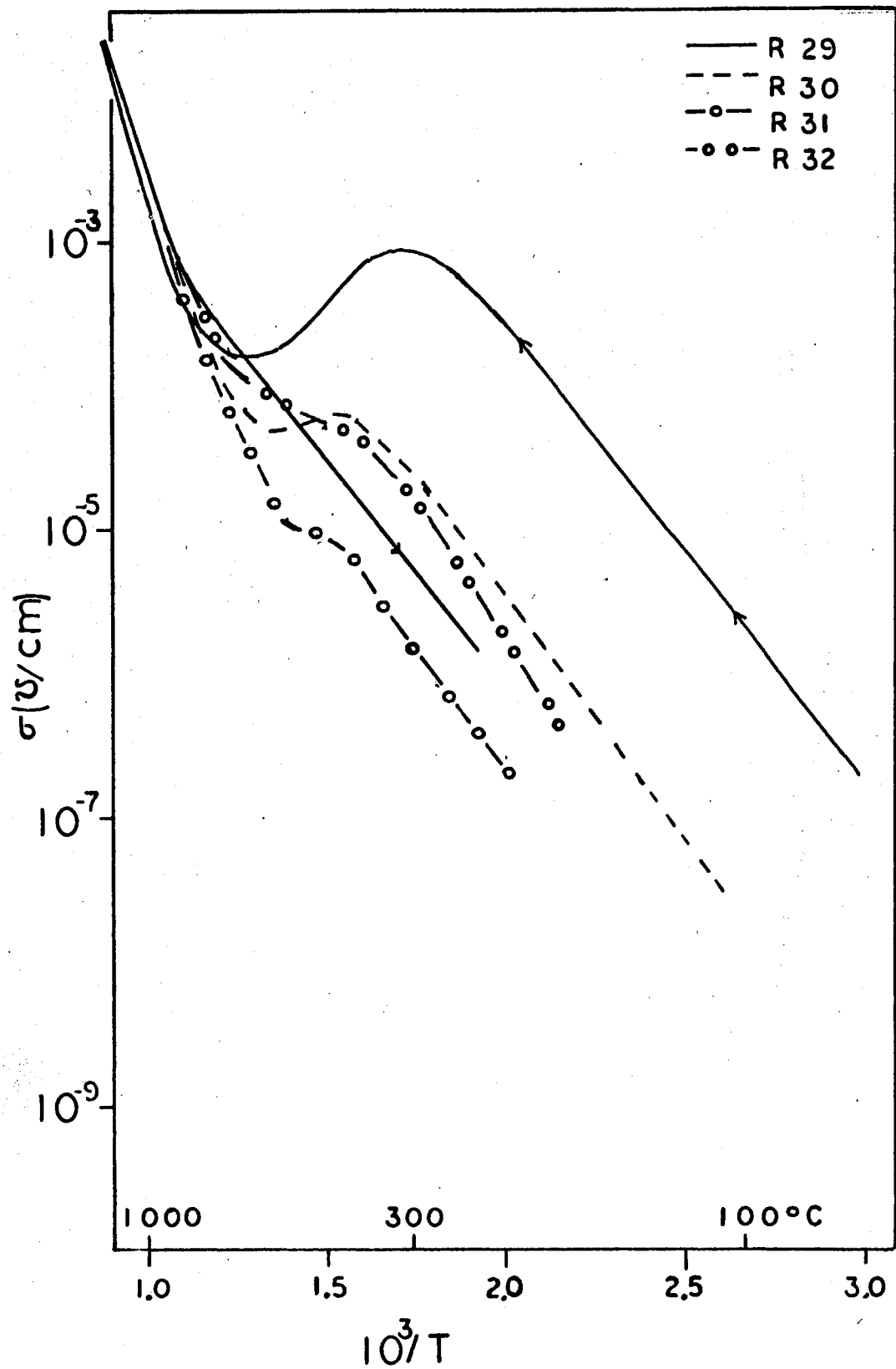


Figure 10. Flash Desorption

ductivity of R-32 is comparable to that of R-30.

From the above it was concluded that the process responsible for the maximum occurs in the dark at room temperature to some extent. The possibility of some gas adsorbing on  $\text{SnO}_2$  was then investigated.

Fig. (11) shows the next series of data. Between R-32 and R-33, S-7 was exposed to the air and light of the laboratory for fifteen days. However, from the beginning of R-33, the sample was kept in desiccated air. Note on the graph the renewed definiteness of the maximum in R-33. Also note that curves R-34 and R-35 are indistinguishable, showing that during the nine days separating them no readsorption had occurred.

The implication of the data thus far is that the heating branch maxima seen in R-29 and R-33 represent the flash desorption of water since it regenerated in damp air but not in desiccated air. Some data designed to fit the flash desorption analysis of Chapter I, as well as adsorption kinetics data, were obtained.

After a certain date no sizeable room temperature irreversible adsorption was observed on any of the several samples that had originally exhibited it. This change could be due to one of the following: (1) some factor (e.g., number of bulk defects) involved in the adsorption may have been gradually "used up" or destroyed by the cycling; (2) some new trace pollutant (either in the air or on the sample surface) may be blocking the adsorption; (3) some pollutant had been assisting the adsorption previously, but after the change, the pollutant was absent. The first possibility is ruled out by the simultaneous change in the several samples with differing histories. The second one suggests experiments in carefully controlled ambient, which are reported in Section B. The third possibility suggests experiments in which the chemical

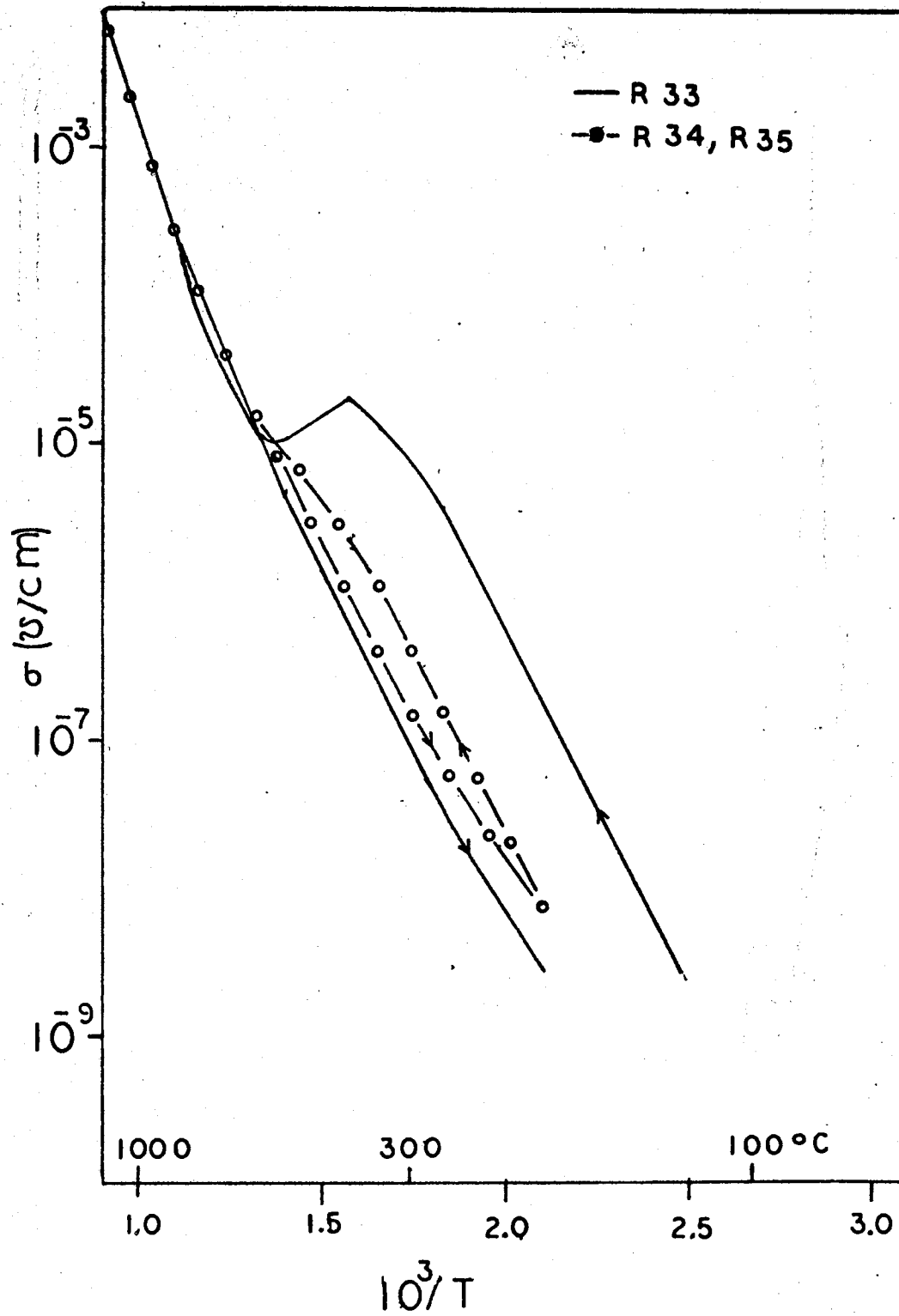


Figure 11. Flash Desorption

potential barrier that had been circumvented catalytically might instead be surmounted thermally.

Some success in taking such high temperature adsorption data can be reported. Flash desorption and adsorption kinetics taken after the change are reported below in their respective subsections. As will be pointed out, however, the observed strength of the regenerated effect is only about one percent of its former value, and qualitative changes have also occurred.

### 1. Adsorption Kinetics

The adsorption kinetics data taken before the change in adsorption character is plotted in Fig. (12). In this figure both current and inverse current are plotted as functions of log time, with  $t = 0$  the point at which moist air was opened to the system. The temperature was about  $300^{\circ}\text{C}$  ( $10^3/T = 1.75$ ). Note that it is the inverse current which is linear.

Figure (13) is a similar plot of data taken after the change in adsorption character for the same sample, S-7. Here only current as a function of log time is plotted since it is clearly linear.

The conclusion to be drawn here can be put in terms of the predictions of Chapter I, Section C. There it is shown that assuming that  $N_a^*$  fits either Eq. (5a) or Eq. (5b) predicts respectively, inverse current or current will be a linear function of log time. Comparison of Fig. (12) and Fig. (13) shows that basic Elovich adsorption mechanism persists, but the change in character of the adsorption is accomplished by a change in the appropriateness of the choice of approximation. Since the value of  $N$  in each case starts from zero, the change in approximation

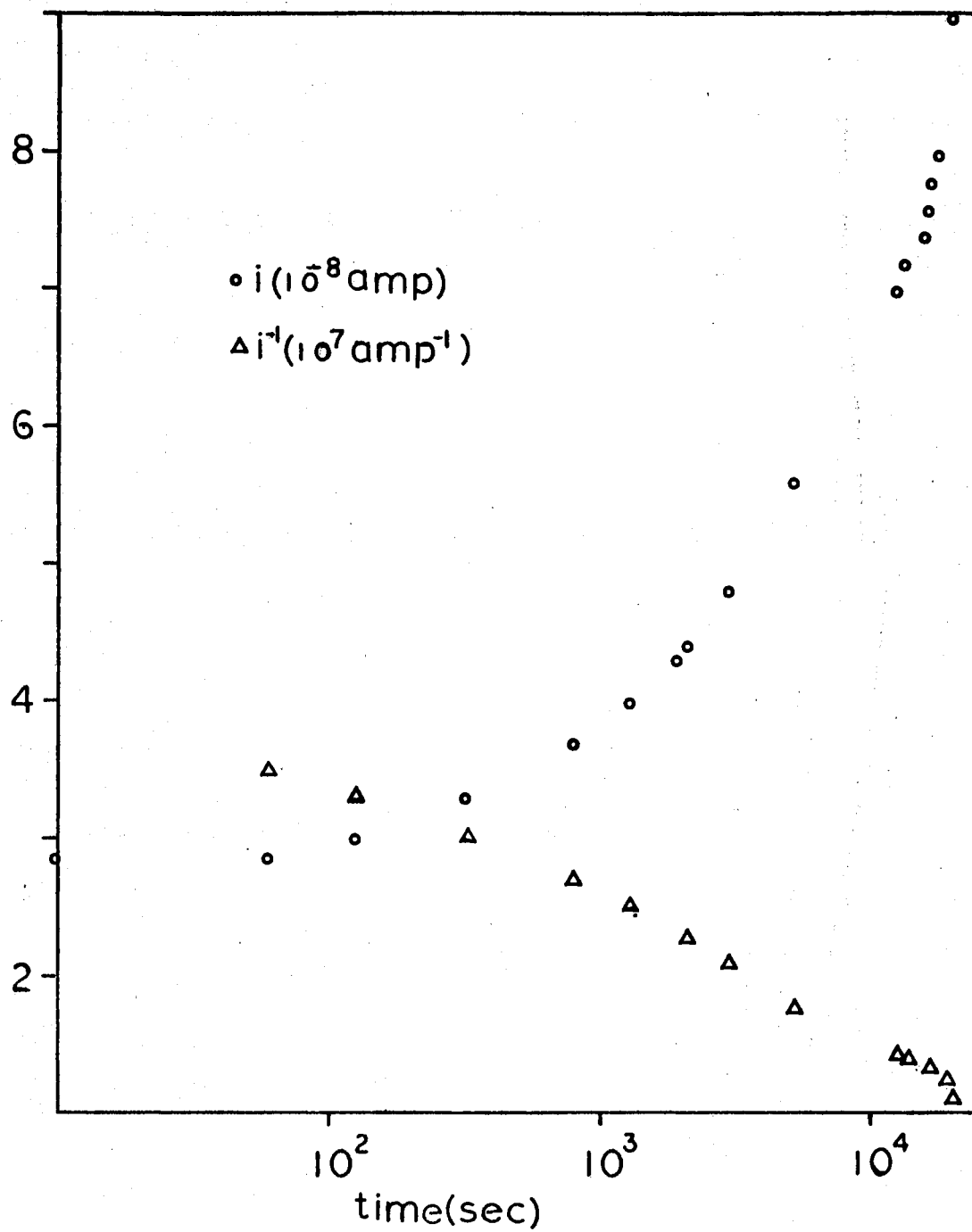


Figure 12. Adsorption Kinetics R-37.

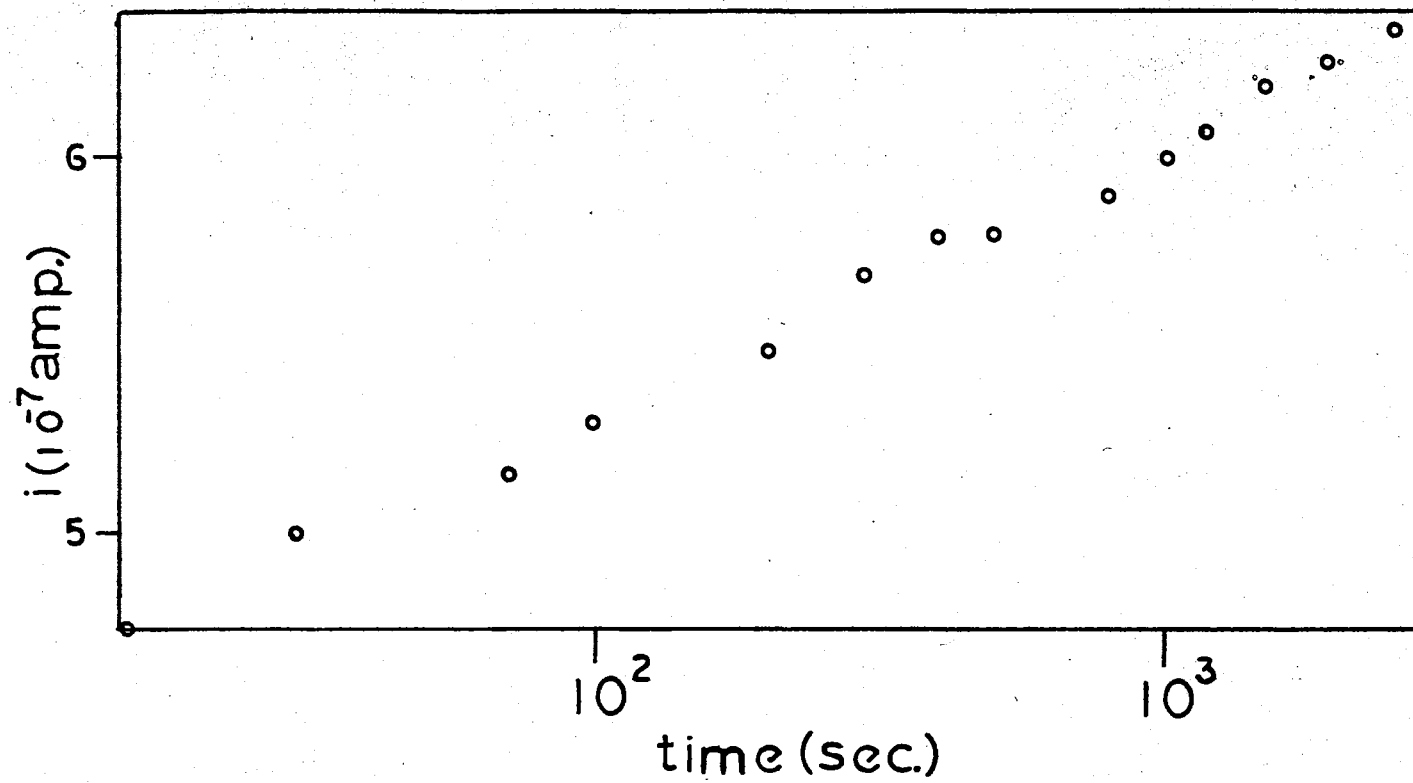


Figure 13. Adsorption Kinetics R-48

choice should be due to some change in  $N_a^*$ . But a comparison of current at various temperatures from the first heating (R-29) to the last run (R-49) fails to show any large change in the magnitude of the current with the sample in the desorbed state. Thus, no evidence of a change in  $N_a^*$  is seen.

## 2. Flash Desorption

Flash desorption data taken to fit the analysis of Chapter I will consist of at least three heating and cooling cycles. Here such a set will be designated by an R-number. The various heating branches will be labeled A, C, E and the cooling branches B, D, F.

The first set is graphed in Figs. (14) and (15). In these two graphs, log conductivity has been plotted against  $10^3/T$ . Branch C was begun immediately at the conclusion of branch B. Branch E started about eight hours after the end of branch D. The identity of branch C to E and D to F is represented by one set of points in Fig. (15).

Note that the conductivity on branch A at  $10^3/T = 1.7$ , which is just before the slope changes, is three orders of magnitude larger than on branch B. Note also that branches C and E show an anomaly not appearing upon cooling, but C and E are identical to each other. That reproducibility is taken as proof that: (1) full desorption occurred during branch A, (2) re-adsorption is negligible or absent, and (3) that the anomaly in branches C and E is not connected with the desorption of  $H_2O^+$  and thus may herein be ignored.

Figure (16) shows  $10^3/T$  vs. time for the heating branches. In order to evaluate  $J$  and the  $b_j$  for use in Eq. (37), the data plotted in that figure is tabulated in Table II, vs. the time at equal intervals

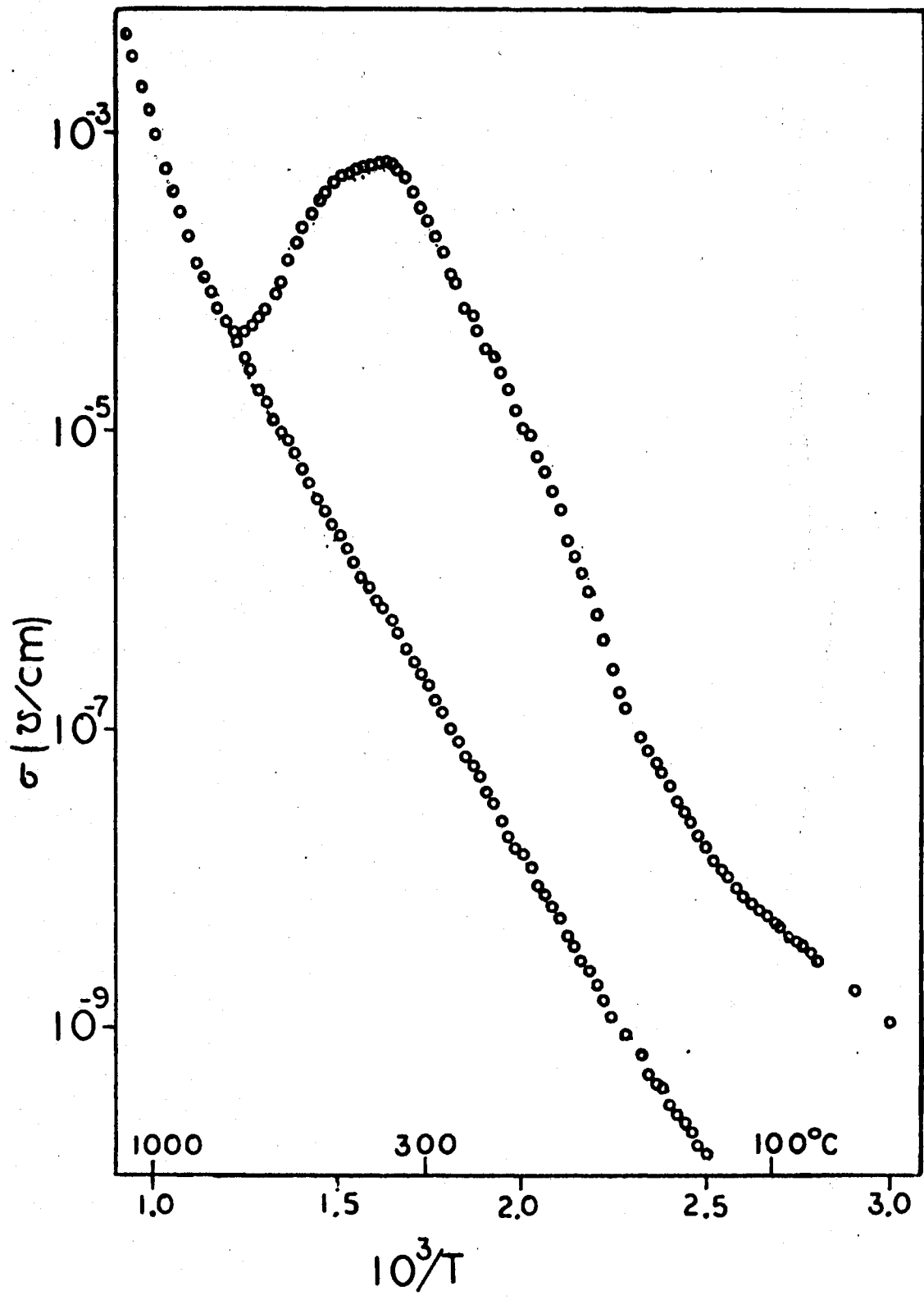


Figure 14. Flash Desorption R-38A, B



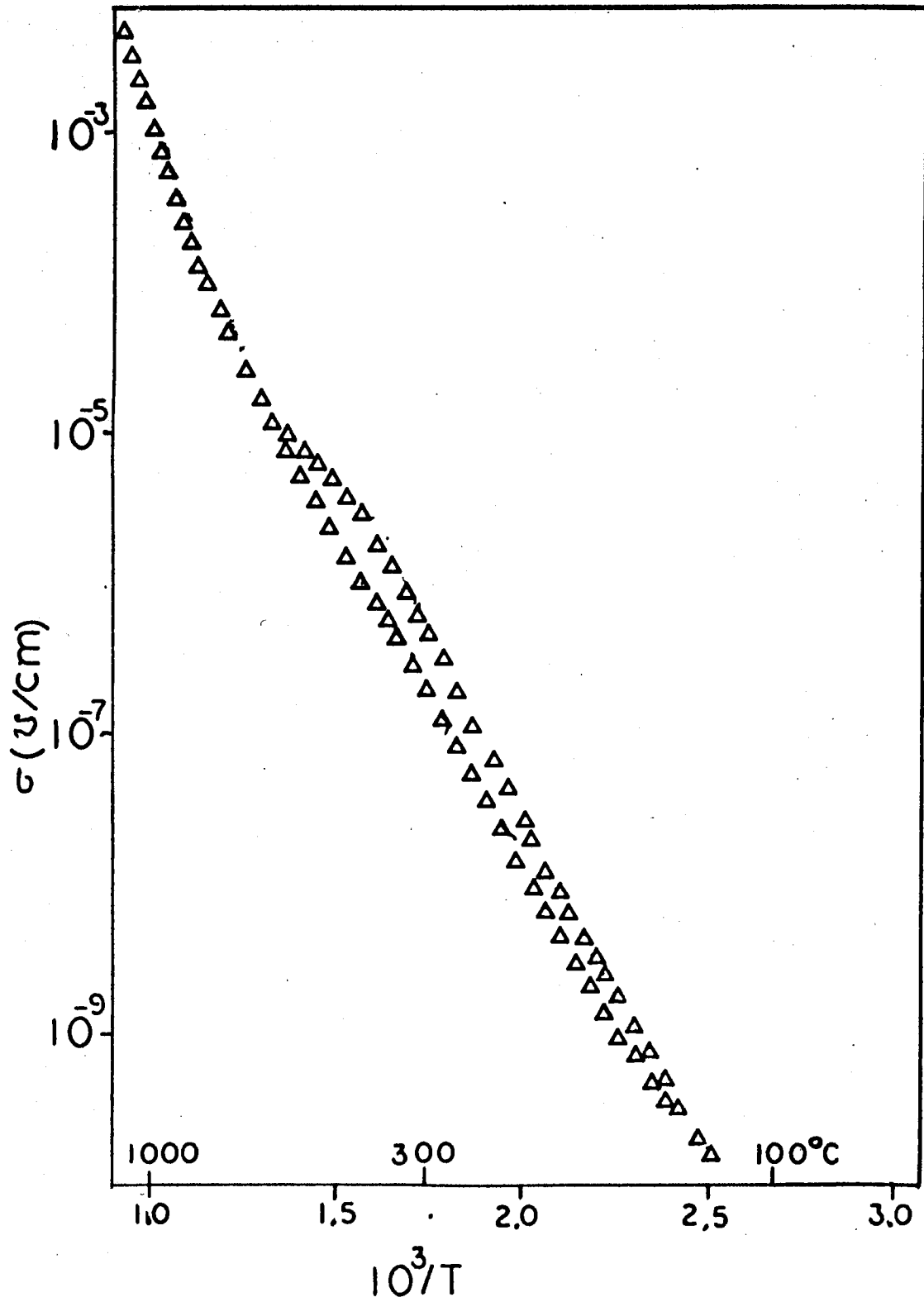


Figure 15. Flash Desorption R-38 C to F

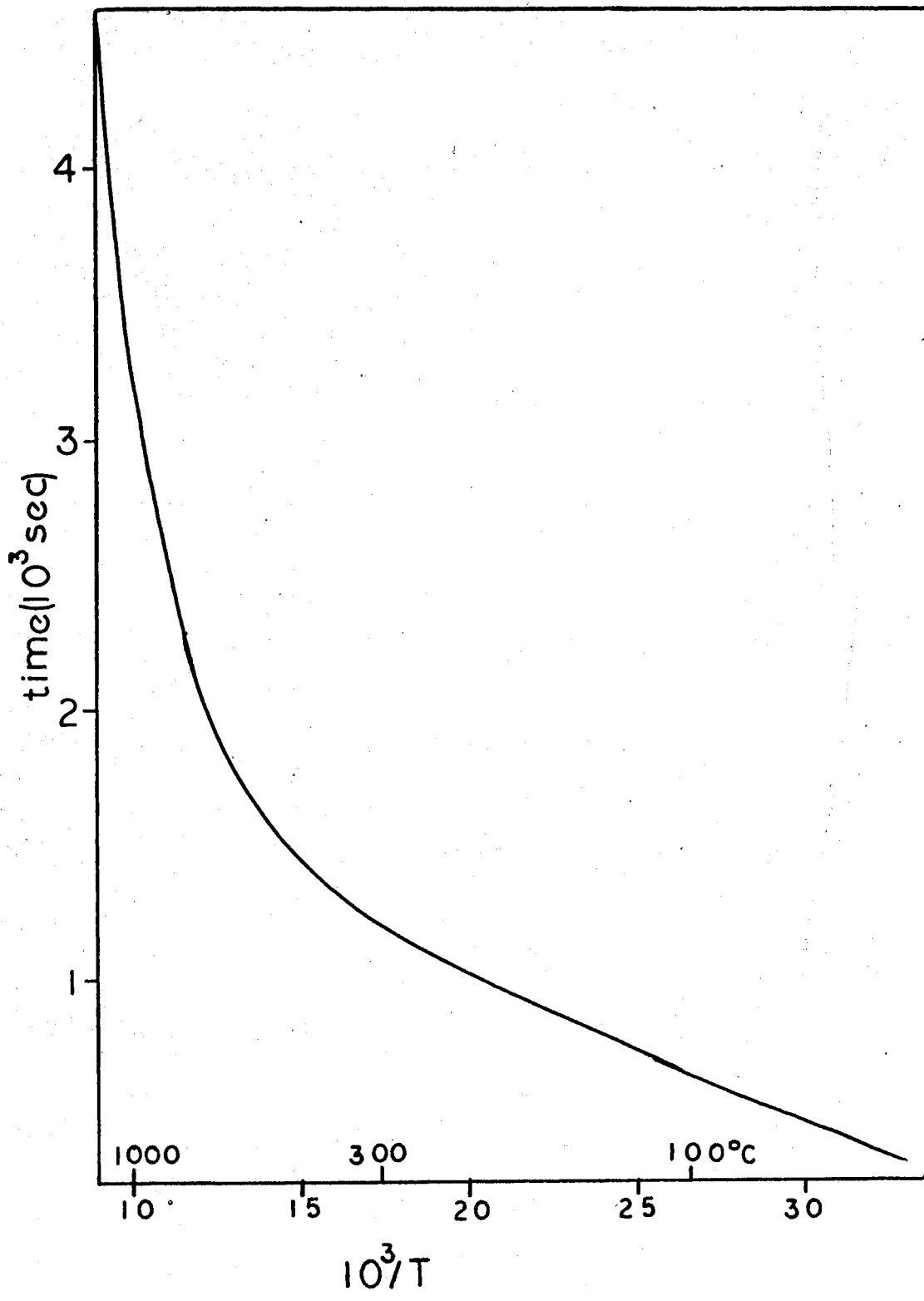


Figure 16. R-38A Time

(0.02) of  $10^3/T$ . Values out to the fifth difference have been tabulated to show the growing effect of noise in the original data. According to reference (32) and (33), the randomness seen in the  $J = 3$  column is sufficient to warrant truncation at that point. Thus,  $J$  is taken as two. Values of the  $\Delta$ 's to compute the  $b_j$  could be taken from Table II, but problems with rounding off error become larger, the further from a reference point a value is computed. So, Table III was made taking the three reference points equally spaced over the whole range of interest.

Using Table III and the Equation

$$f(x) = f(x_0) + \sum_{j=1}^k (\Delta^j f_0 / j! h^j) \frac{j-1}{\ell=0} (x-x_\ell)$$

with  $h = 0.24$ ,  $k = J = 2$  and the  $x$ 's as the  $10^3/T$  values, the  $b_j$  were found by expanding the above polynomial and collecting coefficient of the powers of  $x$ .

Figure (17) shows  $B(x, E_0)$  and  $B(x, E_1)$ . In both cases these are plotted on semilog scales vs.  $10^3/T$ . The  $E_1$  value and how it was obtained will be given below. Beyond that all that is needed to obtain  $B(x)$  and  $B(x, E_1)$  are Eq. (38) and Eq. (37) respectively, and the  $b_j$  as already explained.

The next three graphs, Figs. (18), (19), and (20) show the data of R-38 analyzed by Eqs. (27), (28), and (29) respectively. In each graph the log of  $f(\text{data}; \ell)$  vs.  $10^3/T$  is plotted as the top curve. The next curve in each graph is  $10^6 f(\text{data}; \ell) / B(x)$ , and the third curve is  $10^6 f(\text{data}; \ell) / B(x, E_1)$ . Here the value of  $E_1 = 1.17$  ev was taken from the dominant slope of the  $f(\text{data}; \ell = 0) / B(x)$ . The resultant slope differed less than the limits of precision, thus the iteration process was termi-

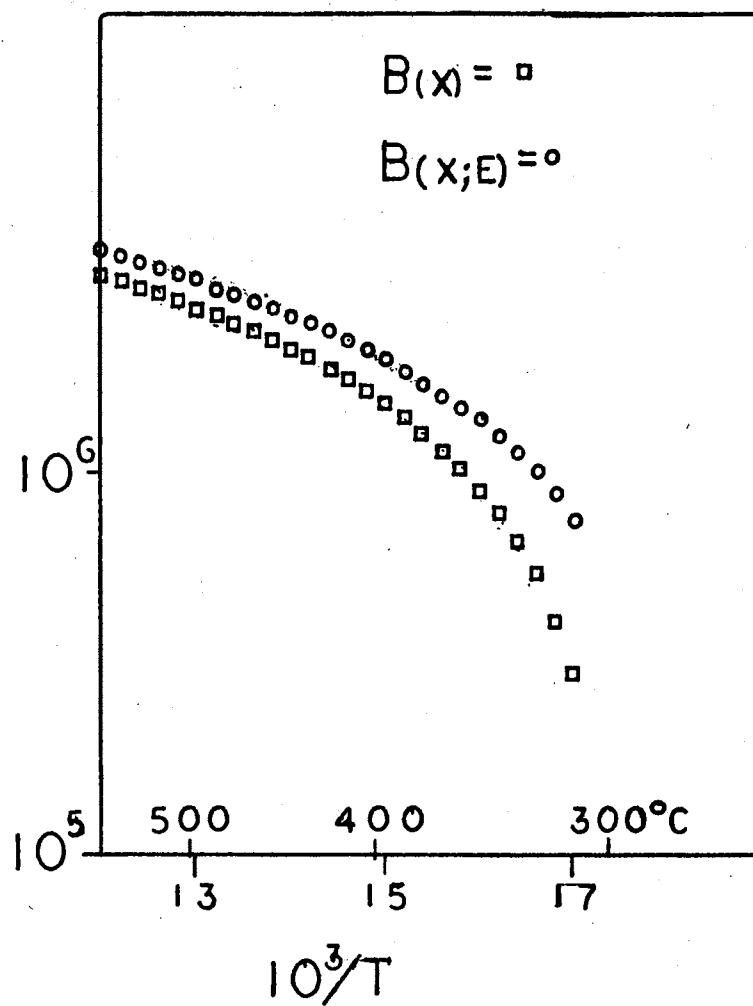
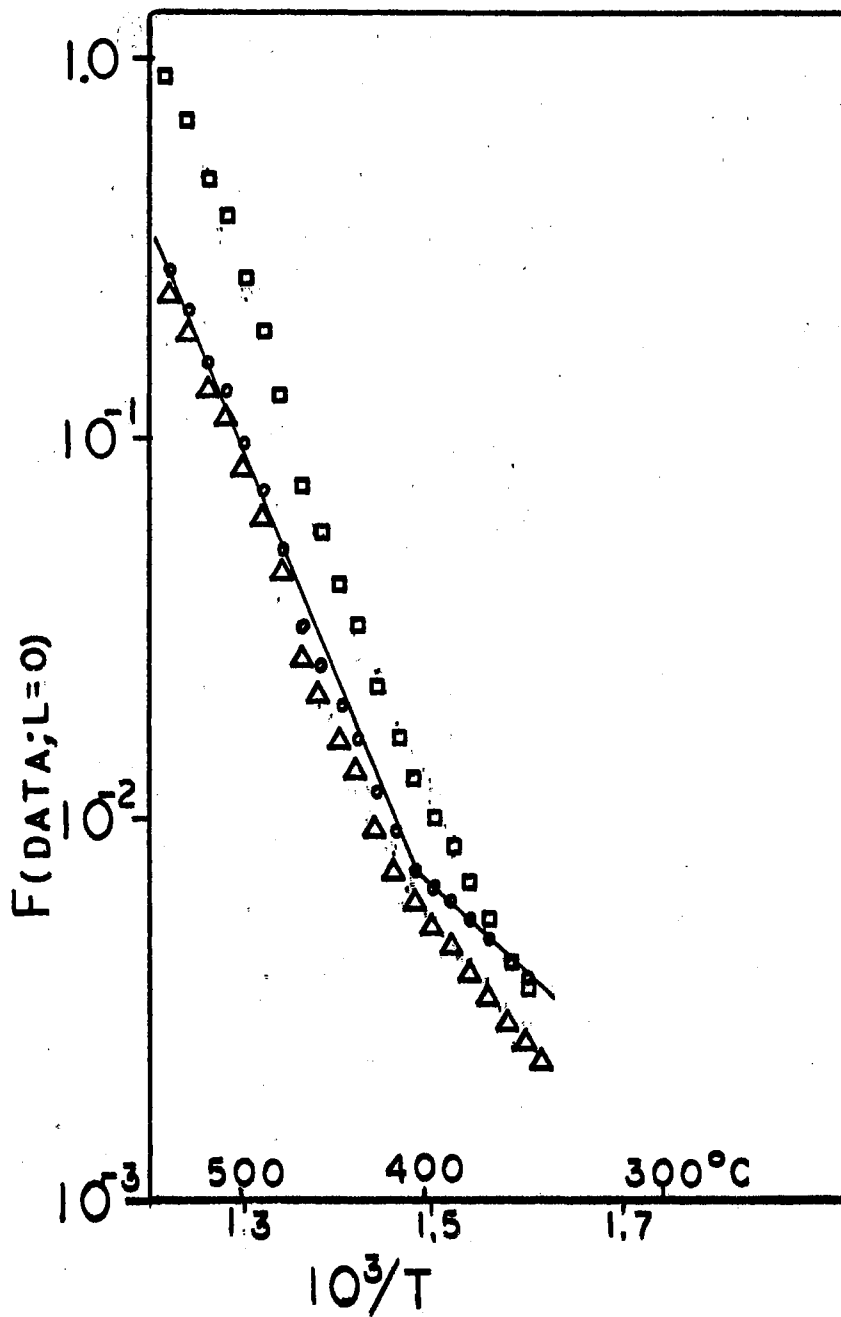
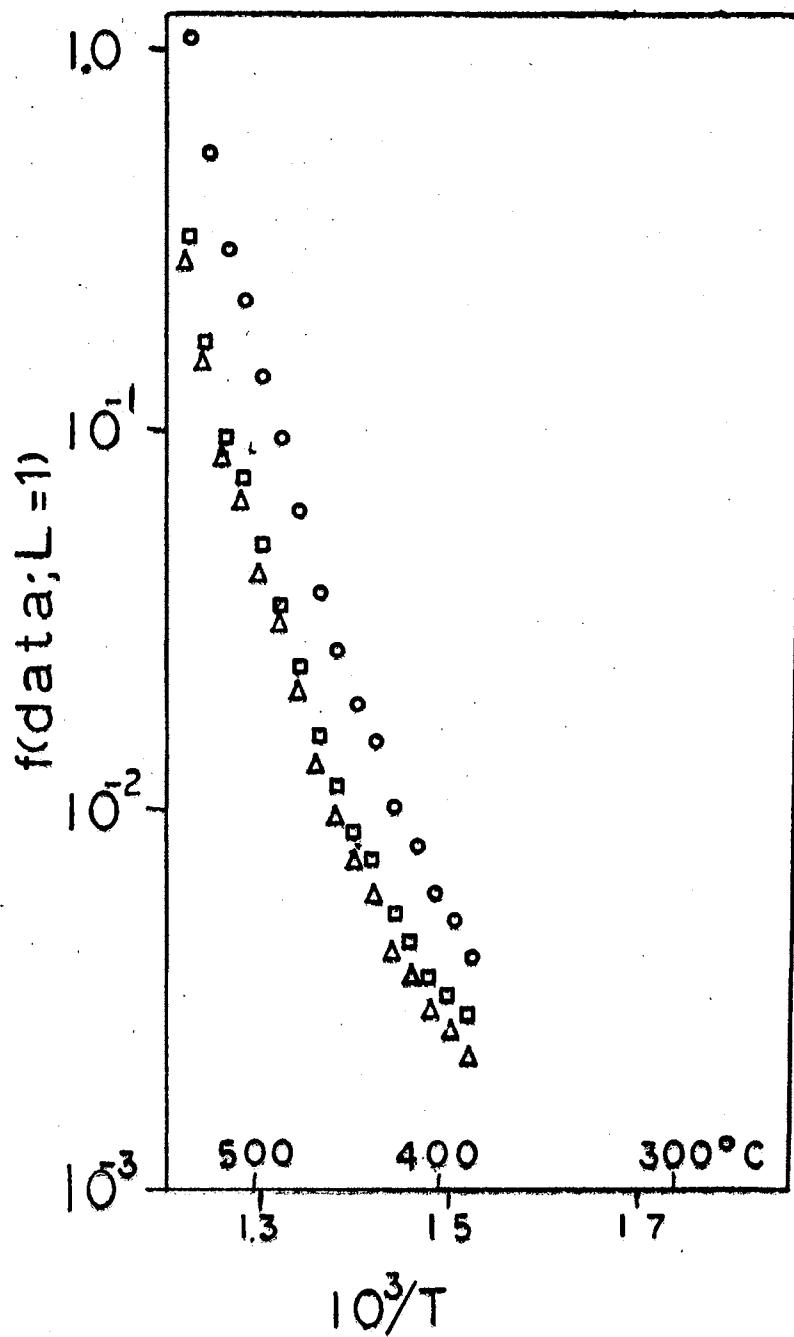


Figure 17. B Functions

Figure 18. R-38 for  $L = 0$

Figure 19. R-38 for  $L = 1$

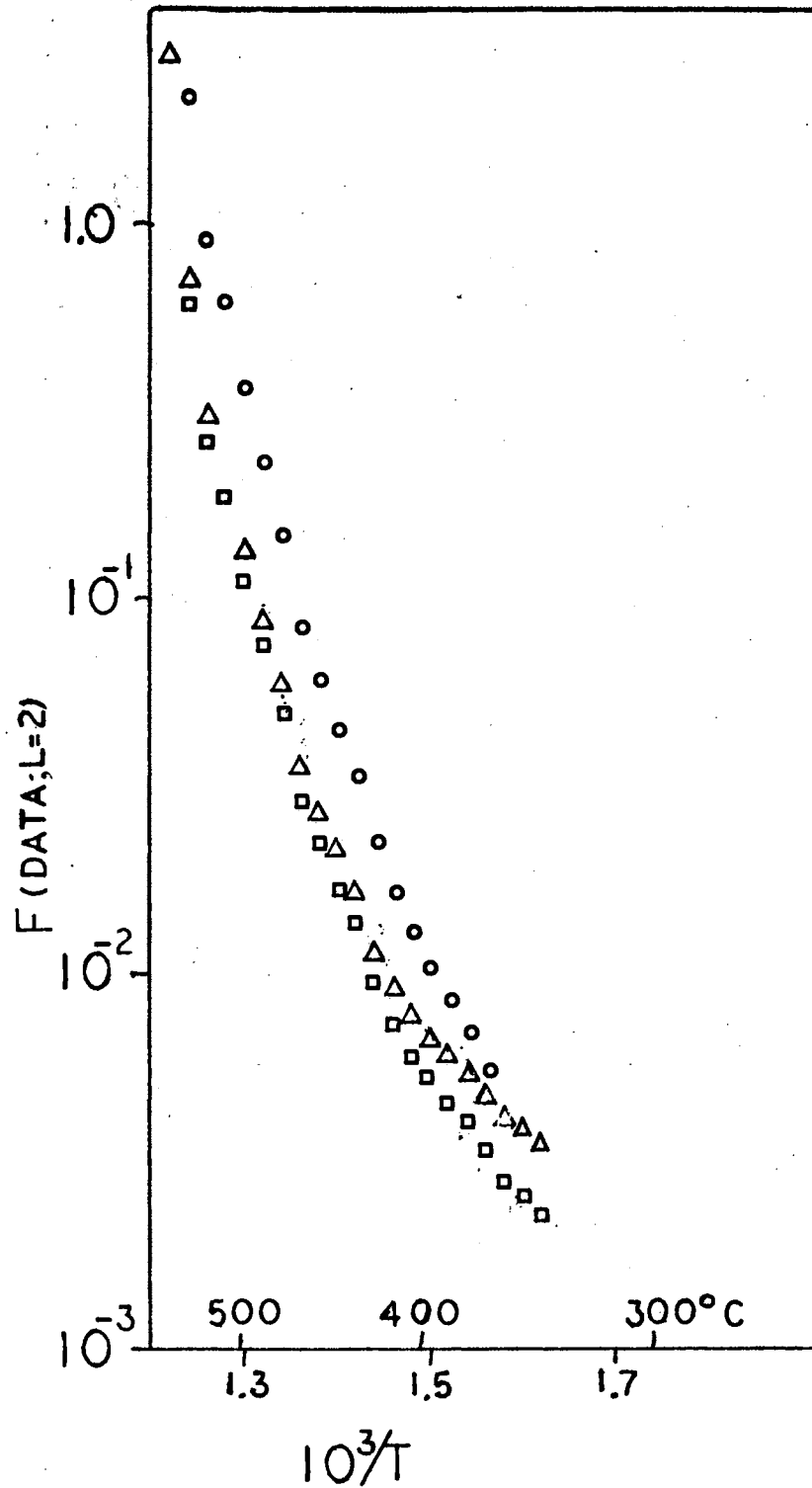
Figure 20. R-38 for  $L = 2$

TABLE II  
DIFFERENCE TABLE

$10^3/T$	t(sec)	$\Delta^1$	$\Delta^2$	$\Delta^3$	$\Delta^4$	$\Delta^5$
1.20	2120	-70				
2	2050	-70	0			
4	1980	-70	0	0	00	40
6	1910	-70	0	40	40	-150
8	1860	-30	40	-70	-110	230
1.30	1830	-60	-30	50	120	-200
2	1770	-40	20	-30	-80	130
4	1730	-50	-10	20	50	-80
6	1680	-40	10	-10	-30	50
8	1640	-40	0	10	20	-40
1.40	1600	-30	10	-10	-20	20
2	1570	-30	0	-10	0	22
4	1540	-30	-10	-10	22	-88
6	1500	-40	22	32	-66	128
8	1482	-18	-12	-34	62	-116
1.50	1452	-30	16	28	-54	84
2	1428	-14	-10	-26	30	-18
4	1414	-24	-6	4	12	-37
6	1384	-30	10	16	-25	38
8	1364	-20	1	-9	13	-27
1.60	1345	-19	5	4	-14	24
2	1325	-14	-5	-10	10	-1
4	1302	-19	-5	0	9	-24
6	1278	-24	4	9	-15	
8	1258	-20	4	-6		
1.70	1236	-22	-2			

TABLE III  
SHORT DIFFERENCE TABLE

$10^3/T$	t(sec)	$\Delta^1$	$\Delta^2$
1.20	2120		
1.44	1540	-580	298
1.68	1258	-282	



nated.

Comparing the shapes of these curves, note that although the value of  $E$  changes insignificantly, the curve itself is noticeably changed from iteration to iteration. The  $\ell = 1$  plot has a visible roundness, but lies very close in value to the two other curves. The  $\ell = 2$  is less curved, but definitely not linear in the upper portion. The lower portion of  $\ell = 2$  is an exact fit to  $\ell = 0$ . The  $\ell = 0$  curve itself displays two quite linear portions with slopes giving  $E = 1.2$  ev and  $0.6$  ev for the upper and lower portions, respectively.

The conclusion the above prompts is that the process has two activation energies, and its "order of kinetics" is zero. The concept of zero order kinetics would at first seem to imply an escape rate independent of the size of the bound population. It is this author's belief that this appearance of having zeroth order kinetics will eventually be traced to complexities in the model and not to such independence. But there is no convincing argument to that effect yet.

Figure (21) contains data taken after the change in adsorption character. Here  $\log f(\text{data}; \ell)$  is plotted using Eq. (27) through (29), with  $\delta = 0.1$ . The use of a finite  $\delta$  is of course dictated by the data (recall from Chapter I  $\delta$  is the inverse of the strength of the effect), and the apparent weakness of the adsorption. The use of a finite  $\delta$  magnifies the scatter in the data.

Note in these curves that there is a new sensitivity to  $\ell$ , with the  $\ell = 2$  curve the most nearly linear.

Figure (22) shows the same data analyzed by Eq. (29B) as of subsection one, above.

Note here that little difference is seen between this graph and the

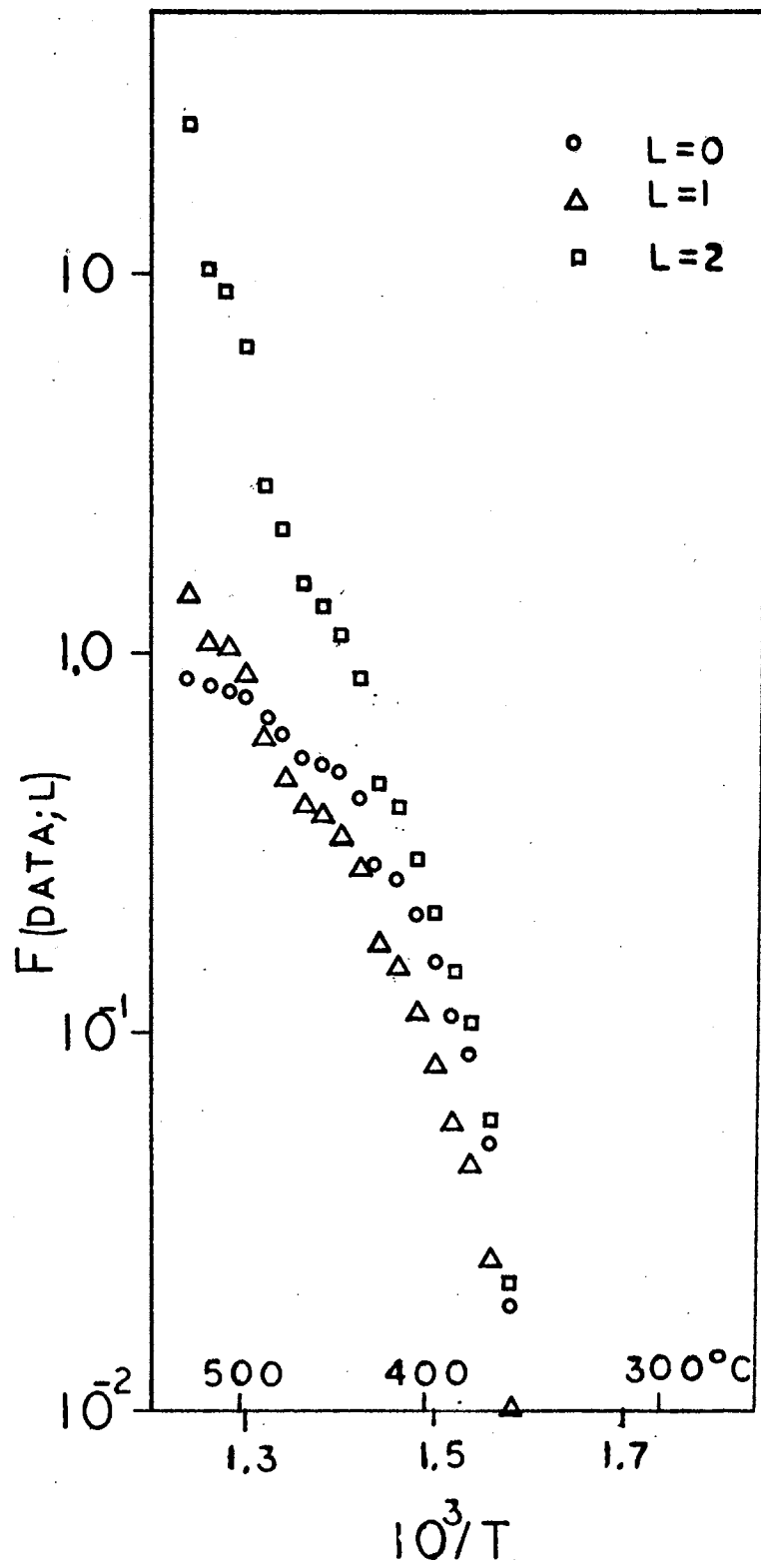


Figure 21. R-49

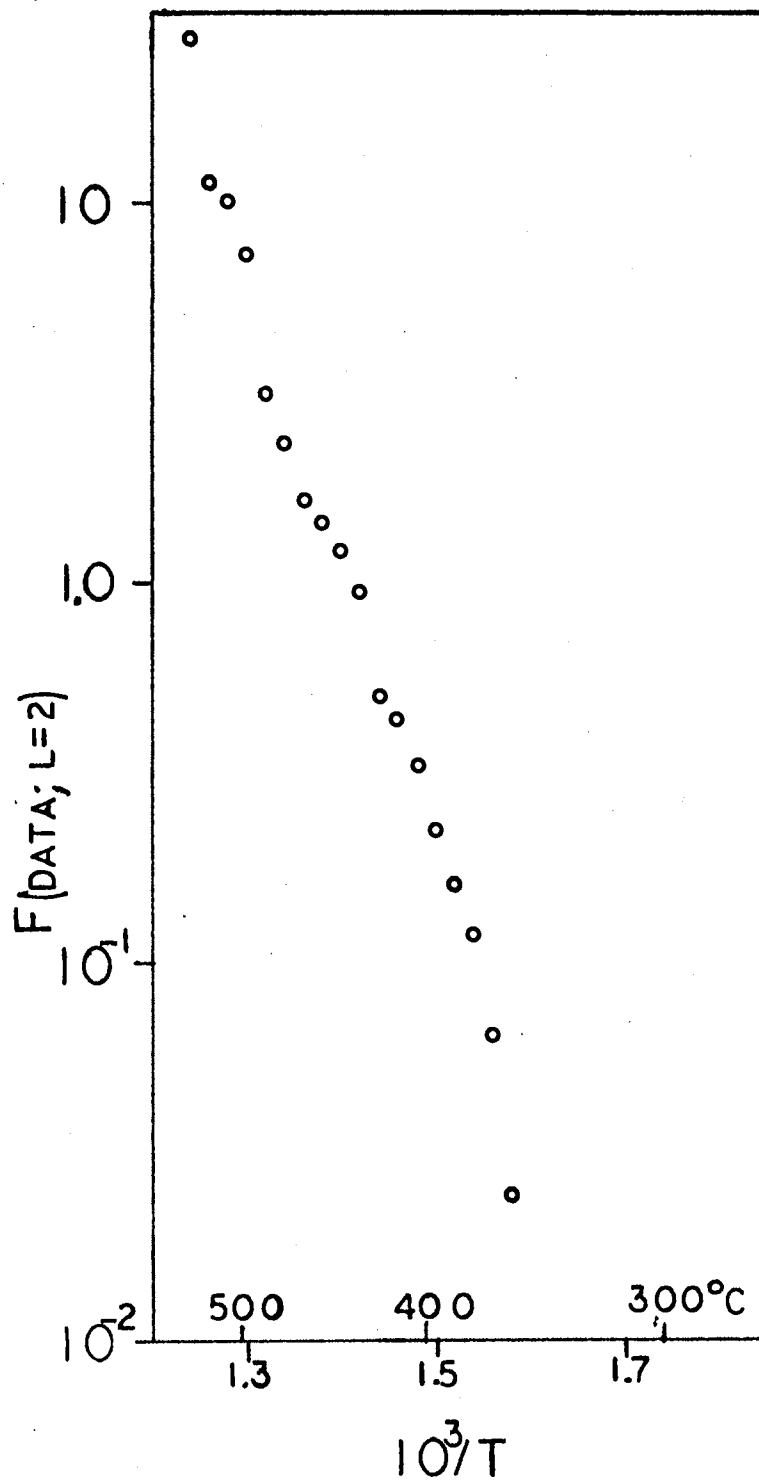


Figure 22. R-49 for Assumption B.

last one, Fig. (21). Although little can be concluded about the appropriateness of approximation, the general trend of the slope is not in contradiction with the slope from which the  $E_1$  value above was found.

#### B. Low Temperature Adsorption

In Section A, above, three possible explanations for the adsorption character change are set forth. Two of them were discussed in that section. The remaining one involves or suggests work with the adsorption which occurs reversibly at room temperature, and that is the subject of this section.

Specifically, the possibility to be herein confirmed or not is that the adsorption change is due to a new pollutant in the ambient, which in some way, blocks the process of room temperature irreversible adsorption. This would have been confirmed if irreversible adsorption had been observed in the presence of only bottled  $O_2$  and  $N_2$  and U. V. None was so observed. Sizable adsorptions were observed, but in each case they proved completely reversible, fully desorbing when the sample was exposed to dry nitrogen.

The tests were run in the F-Probe at temperatures from 20 to 100°C. Ambients consisting of  $N_2$  bubbled through distilled water both with and without the addition of bottled oxygen were tried both in the presence and absence of U. V. radiation (see Chapter II for source details). These various combinations were tried at many temperatures in the range, as well as with temperature increasing or decreasing.

Although no end within the scope of this present work would be served by cataloging all the runs each giving negative results, the following is parenthetically offered as an example for definiteness.

The sample, mounted in F-Probe, showed a change from  $i = 10^{-12}$  amp to  $3 \times 10^{-10}$  amp on admission of  $N_2$  bubbled through distilled  $H_2O$ . The temperature was maintained at  $25^\circ C$ . U. V. at this point raised  $i$  by 30%. After 7 ksec U. V. was shut off, and  $i$  fell 30%. The run was concluded by flushing the system with dry  $N_2$ , at which point the current fell to its original value showing that irreversible adsorption had not occurred in observably large amounts. After each such trial, the conductivity returned to its original value when the sample was flushed with dry nitrogen, showing no irreversible adsorption.

Efforts have been made to perform flash desorption experiments with water reversibly adsorbed at room temperature. The difficulty here is finding a  $T_0$  at which the adsorption is no longer reversible, in order to be able to flash desorb into a dry ambient. Fig. (23) shows the results of a run begun at  $250^\circ K$ . Even at this low temperature flushing with dry  $N_2$  desorbed the water, so the data of Fig. (23) was taken with water present as the temperature increased. At the highest temperature, the wet  $N_2$  was replaced by dry  $N_2$ , with no visible change, showing that all the moisture had been thermally desorbed.

Note the rising slope from  $10^3/T = 4$  to 3.5. This is taken as an indication that the partial pressure of water is here rising, probably due to revaporization of water condensed on the walls of the sample holder. An analysis of the type applied above in Section A-2 is inappropriate here since the assumption of negligible re-adsorption is not here fulfilled. It is concluded that flash desorption for the low temperature range adsorption is not feasible with the equipment presently available.

Another type of data taken was adsorption at equilibrium. Designed

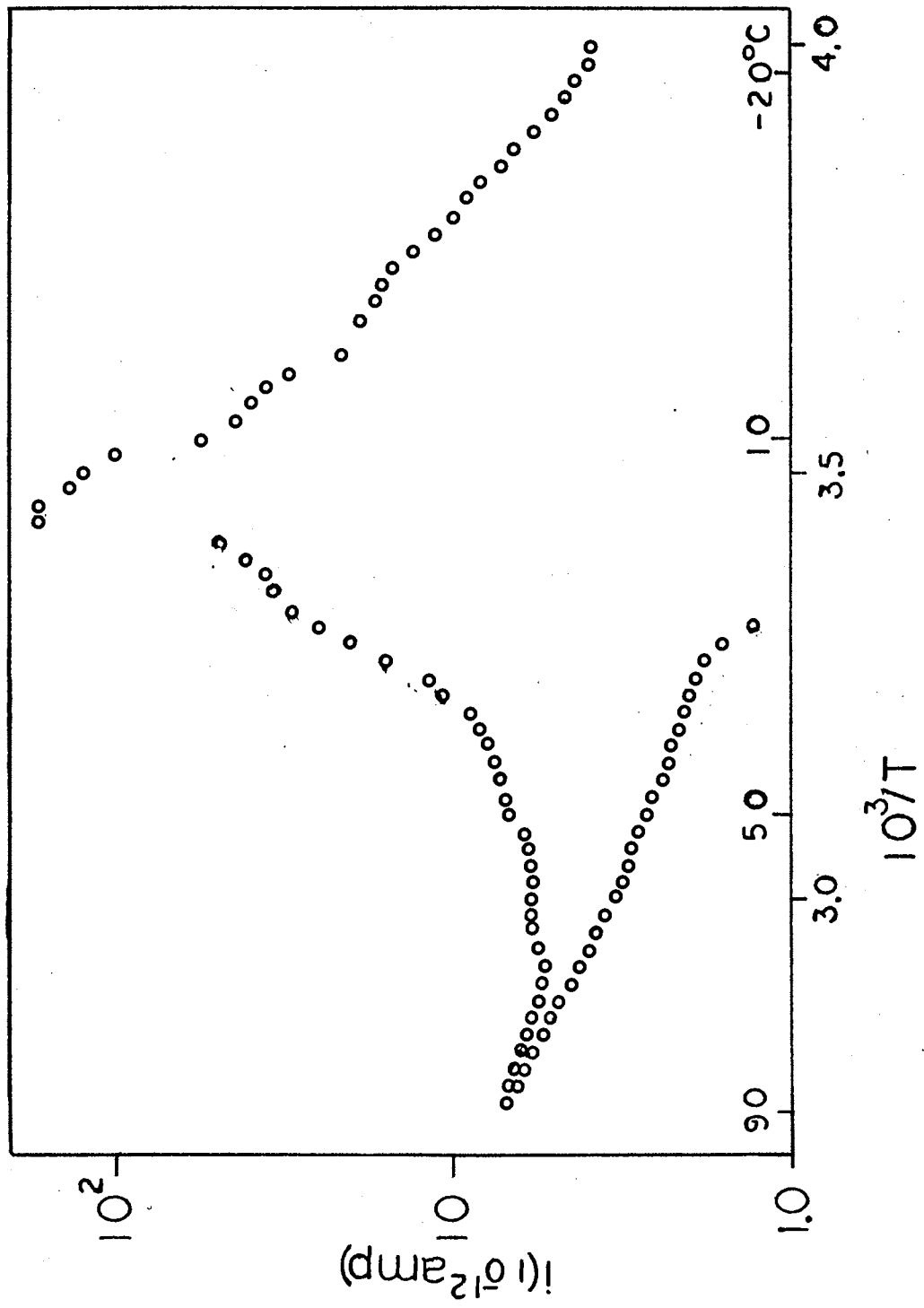


Figure 23. Low Temperature Desorption

to fit the analysis laid out in Section B of Chapter I, Eq. (12) such data could yield the quantity  $\Delta E = E_d - E_a$ , the difference between desorption and adsorption energies.

Figure (24) shows current taken at various equilibrium temperatures in an ambient of  $N_2$  which had been bubbled through  $H_2O$  before the run. Temperatures remained constant at these points for times from one hour to twelve hours. The open circles represent points taken at equilibrium upon increasing the temperature, and the filled-in circles are points taken on the way down. Suggestions for improving the pressure stability and other problems encountered are described in Section C, below.

Figure (24), as seen in the light of Eq. (12), consists of lower temperature portions reflecting the various amounts of adsorbed water, and high temperature portions due to bulk effects. The lower temperature portions of the two curves are essentially parallel and their slopes indicate a value for  $\Delta E$  of the order of one and a half electron volt.

### 1. Adsorption Kinetics

Since (as the above subsection showed) no irreversible adsorption occurred in wet nitrogen, the adsorption kinetics of the reversible process could be studied. A series of data taken on sample S-22 (see Table I) is reported in Fig. (25) through Fig. (30). In each case the sample remained at room temperature, and  $t = 0$  is taken at the instant the previously evacuated system is opened to ambient. For Fig. (29) the ambient is water vapor alone. For the others, ambient was  $N_2$  bubbled through  $H_2O$ . Fig. (25) and (26) show inverse current as well as current. In both figures it is seen that it is the current plot which has portions that are linear in log time thus following Eq. (16B) instead of

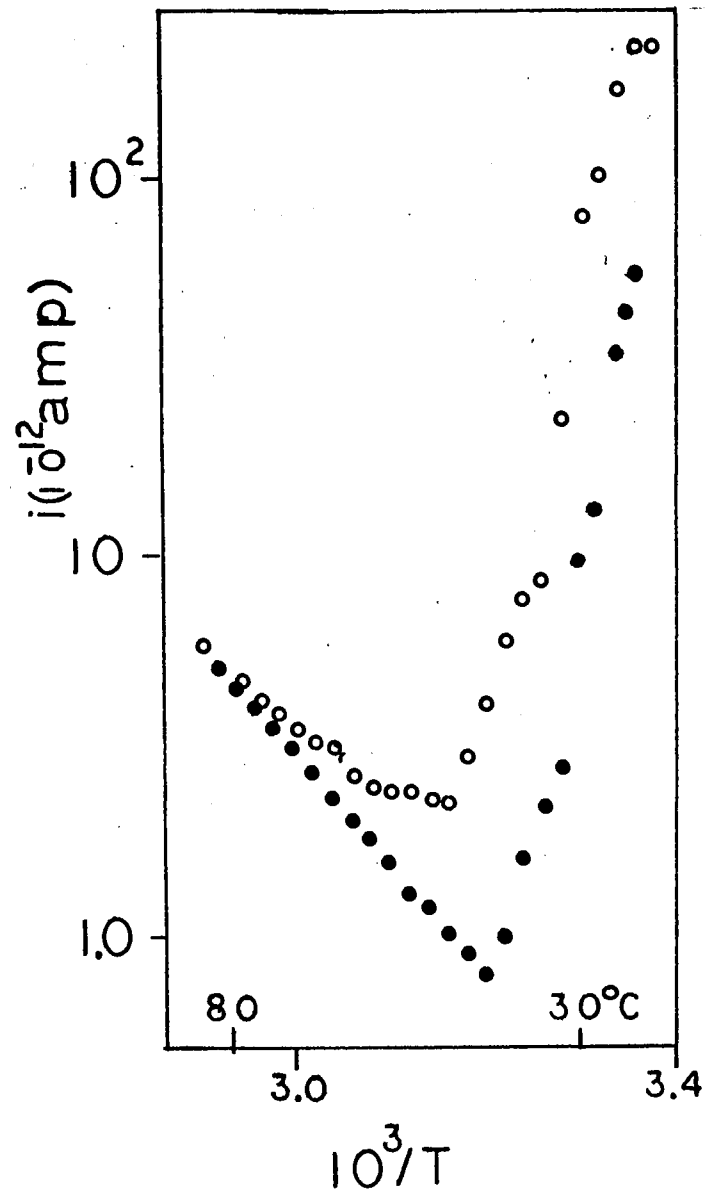


Figure 24. Equilibrium R-44



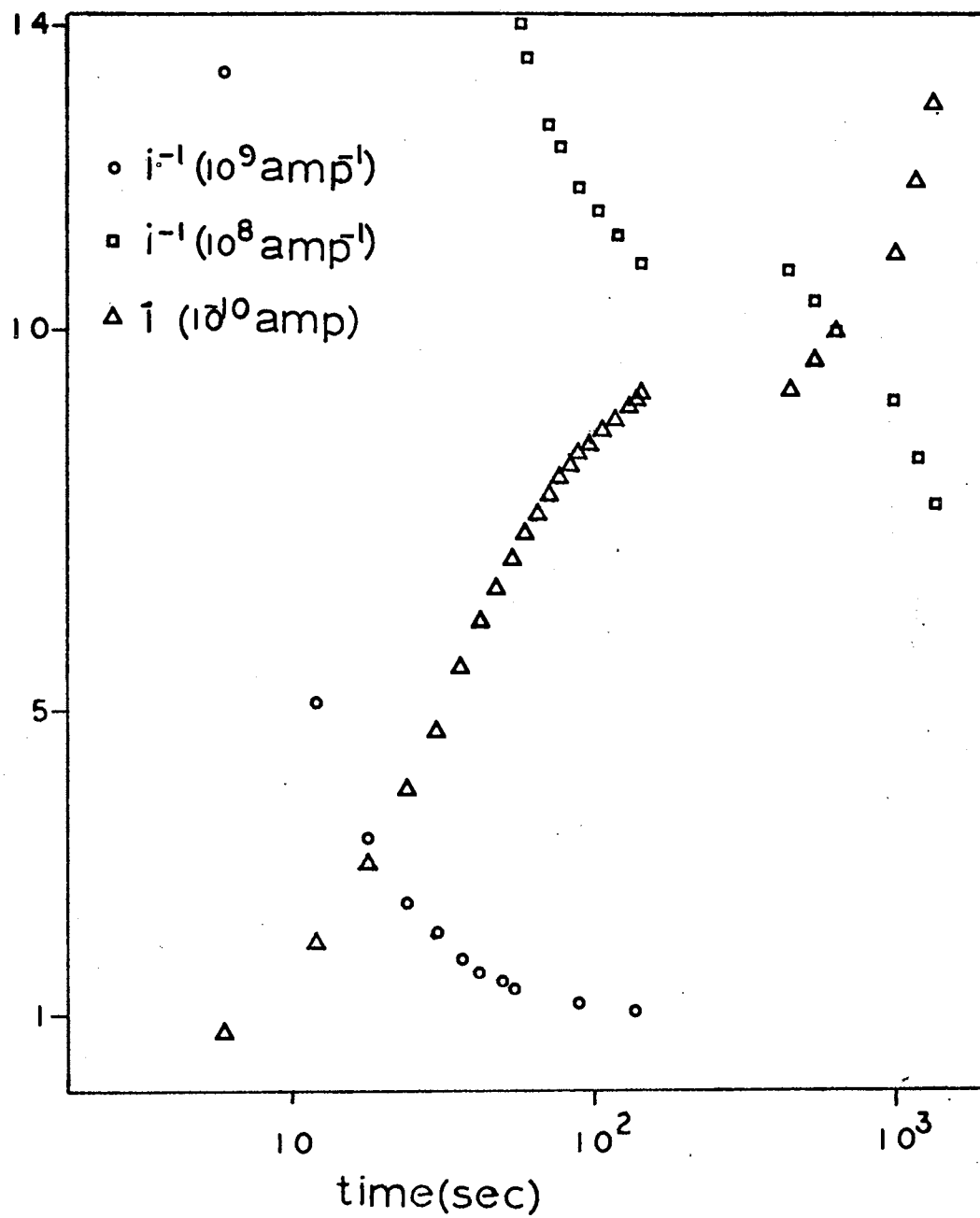


Figure 25. Adsorption I

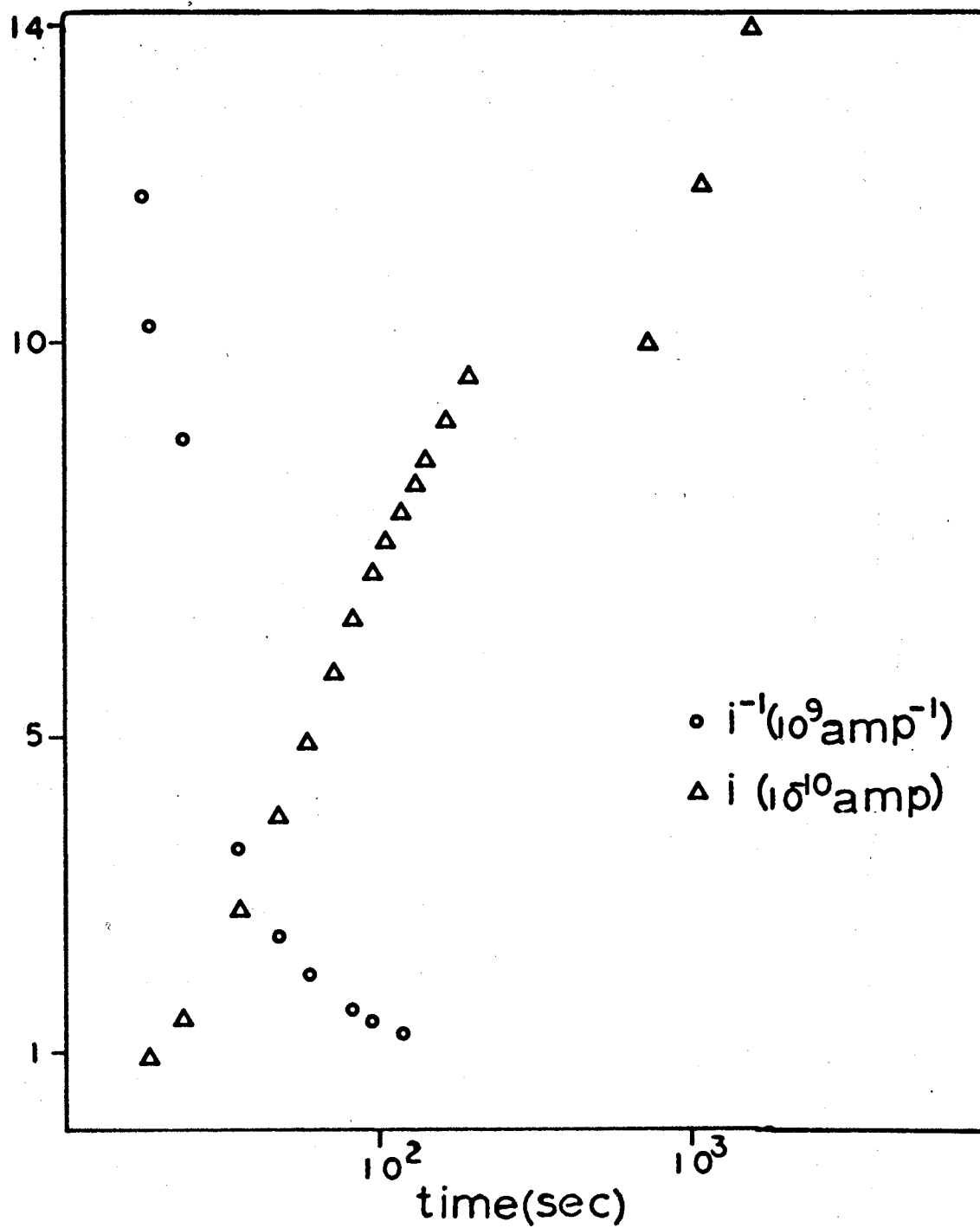


Figure 26. Adsorption II.

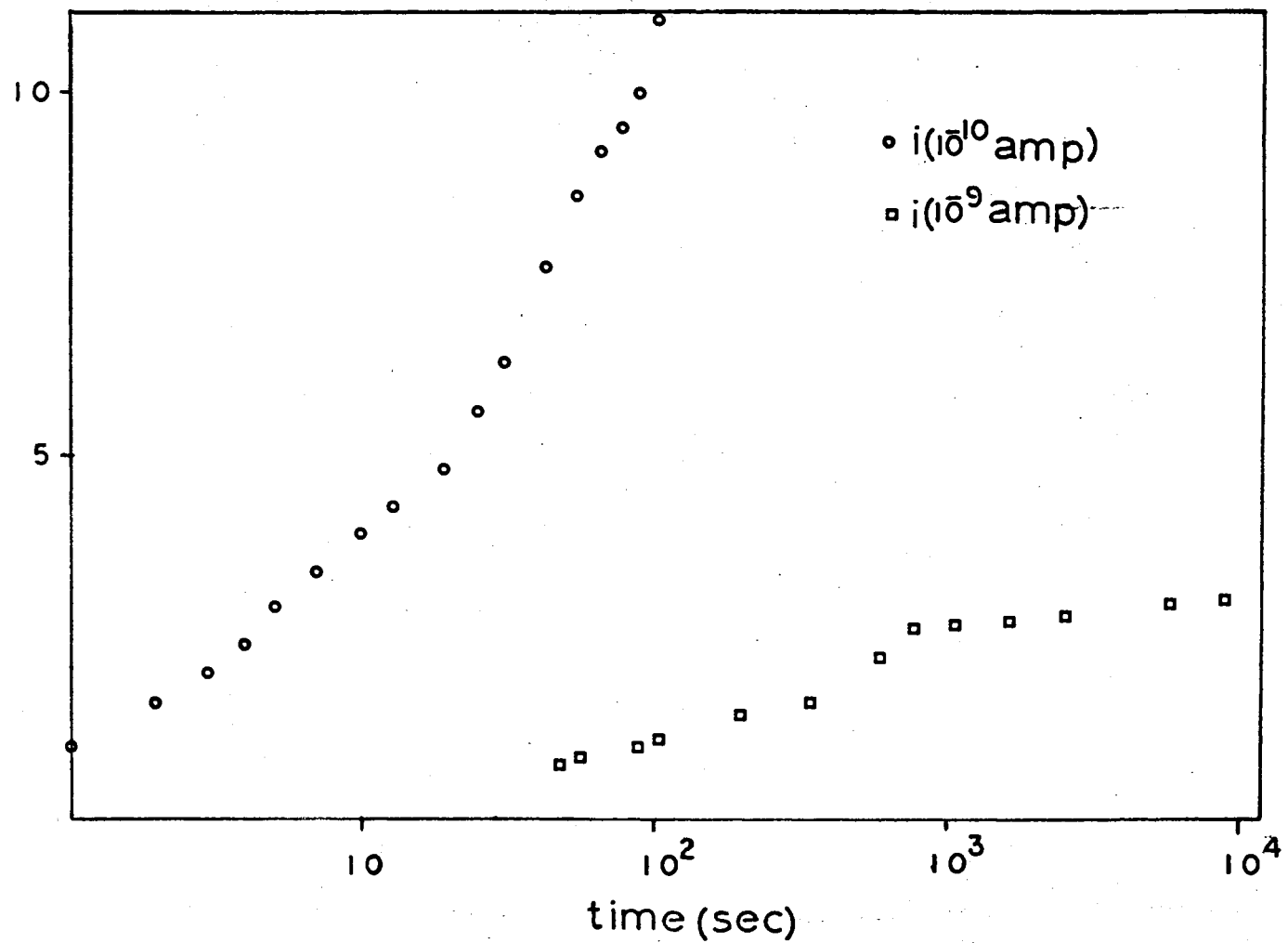


Figure 27. Adsorption III

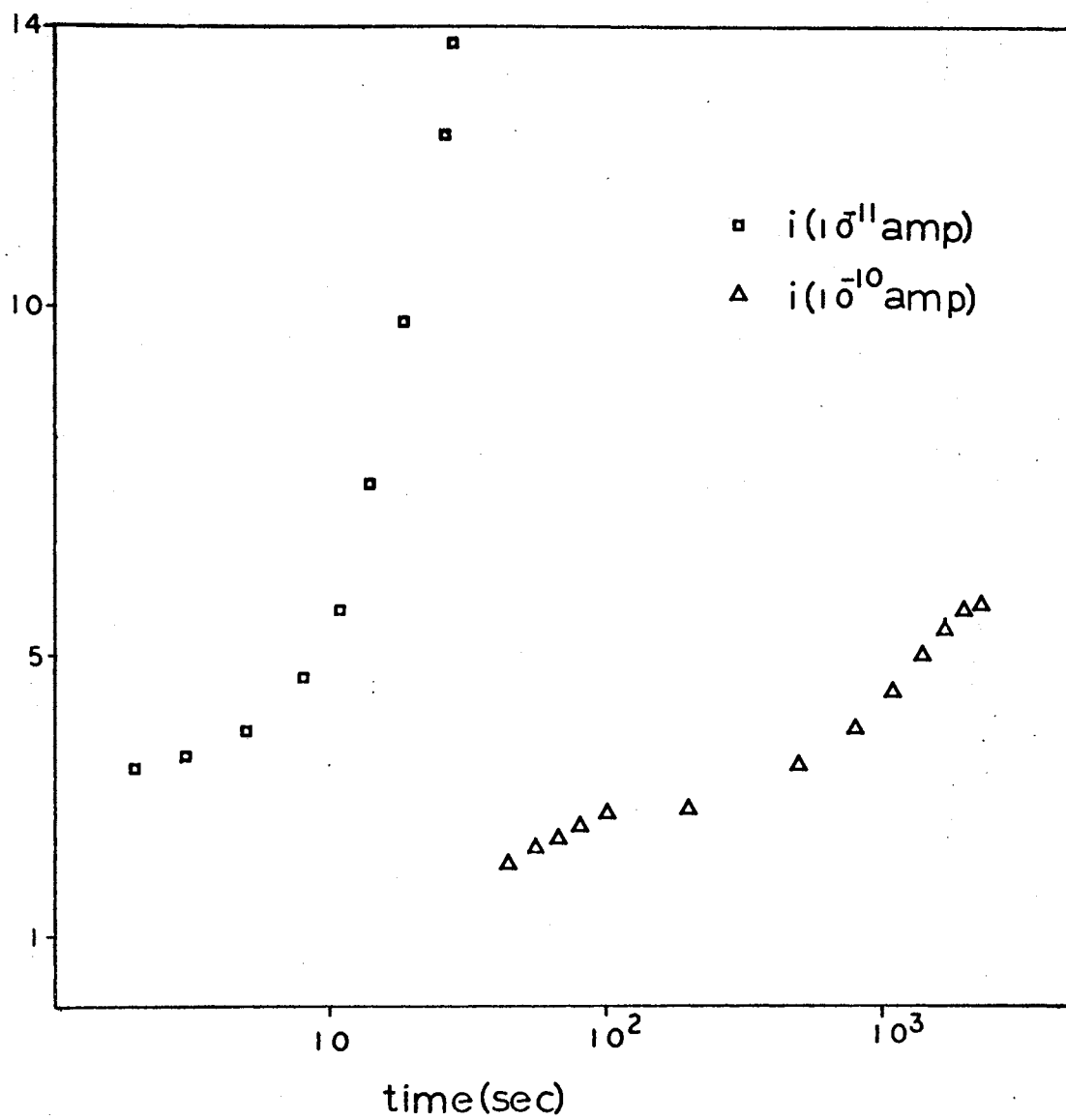


Figure 28. Adsorption IV

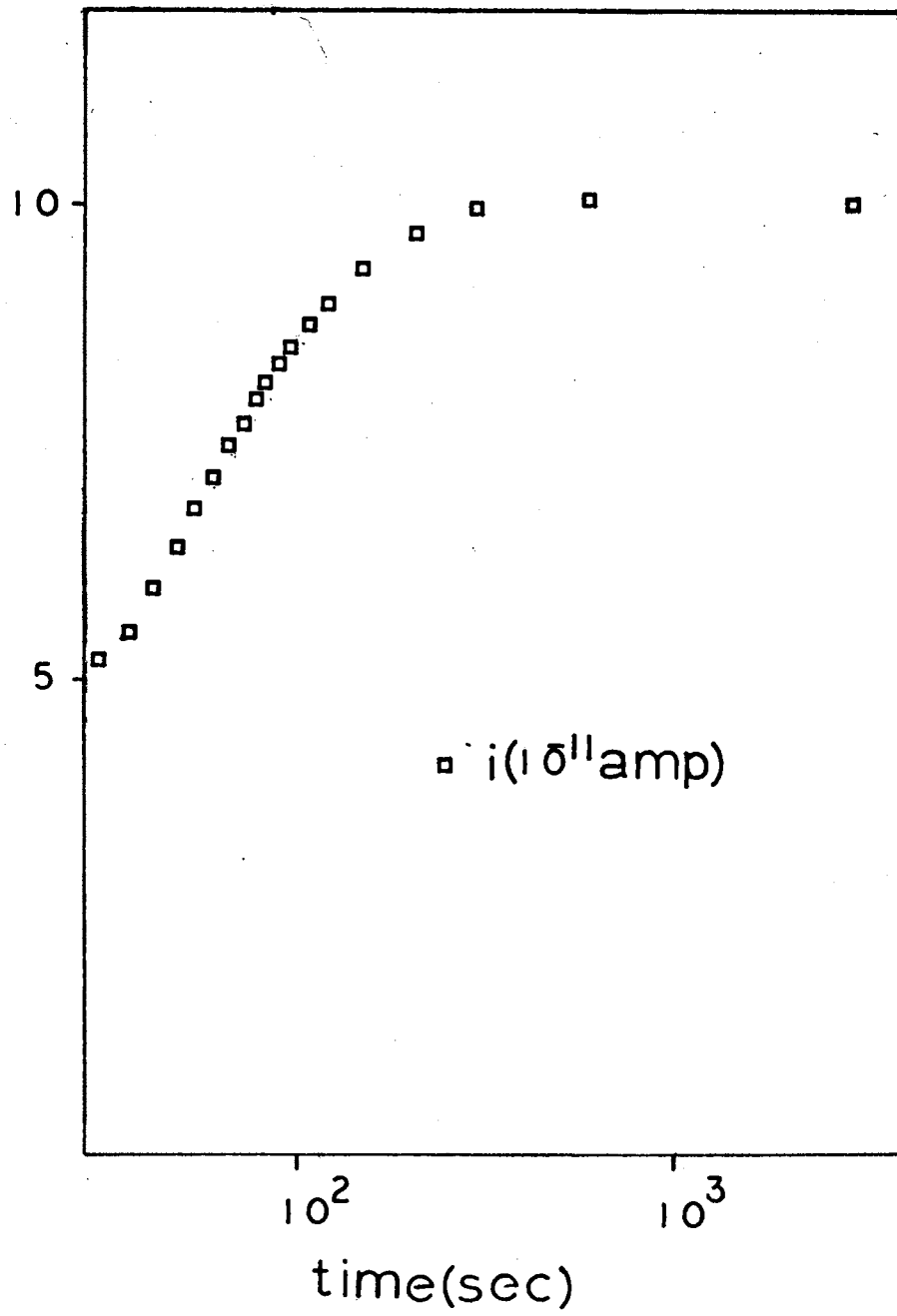


Figure 29. Adsorption V

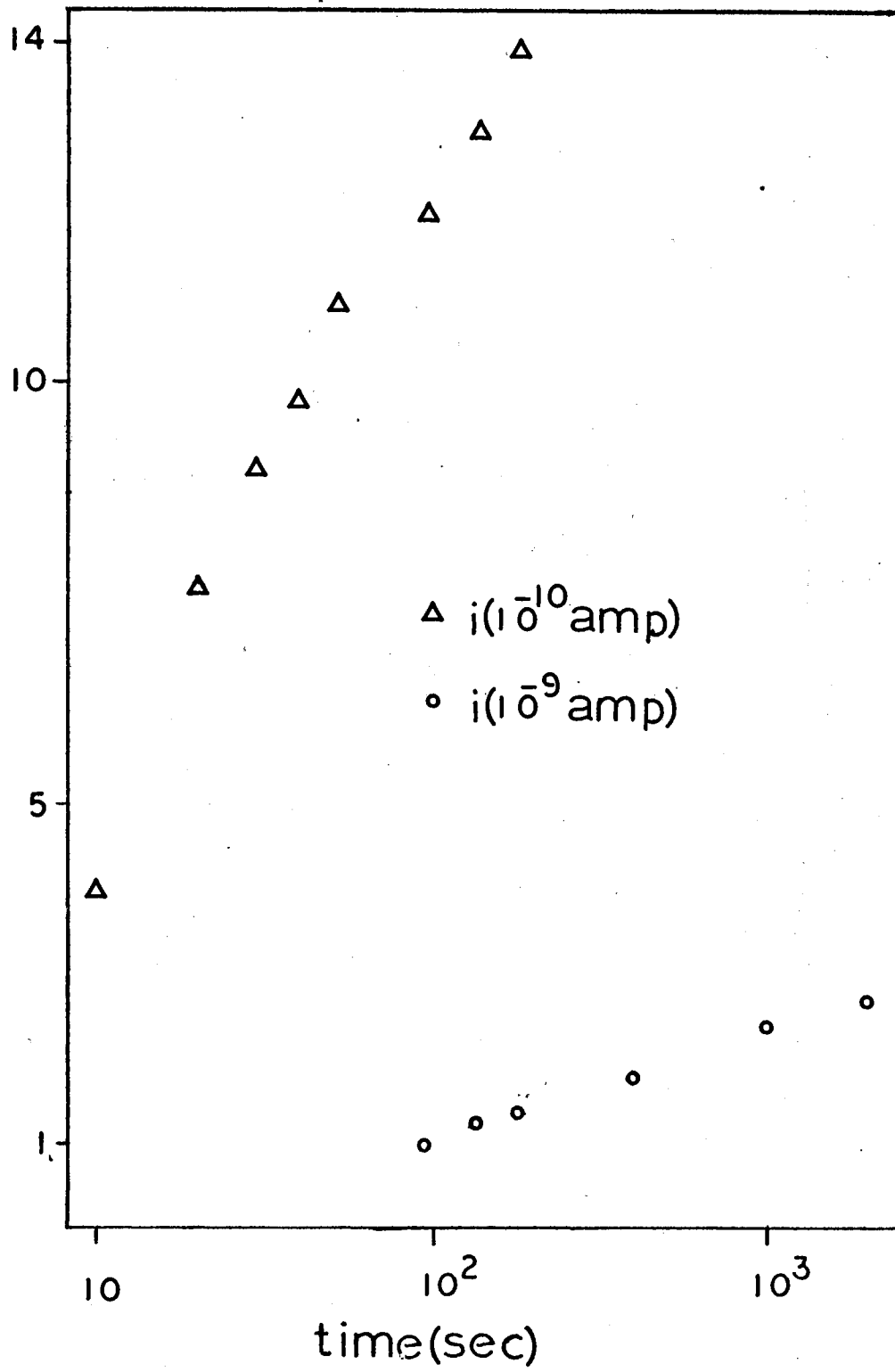


Figure 30. Adsorption VI.

(16A) and favoring the corresponding choice of assumptions. In subsequent plots inverse current is not shown.

Although the current curves do show linear regions, they are not neatly reproducible. This series is given in the order taken, and random fluctuations can be seen by comparing currents at a single time (say fifty seconds). Such fluctuations are taken as a result of the difficulty in controlling the water content of bubbled  $N_2$ .

Further note the plateau that occurs in Figs. (25), (26), and (28) in the range around 200 sec. This appears to be associated with a transition to a slower process, but a definite conclusion must await further work.

Comparison of Fig. (29) with the others shows again the initial linear behavior, but the final current is far below the others. That is taken as indicating that a smaller  $p_{H_2O}$  is achieved by opening the system to water than by bubbling  $N_2$  through  $H_2O$ .

### C. Suggestions for Further Study

In this section a number of ideas will be proposed for further work. Problems that have been overcome, as well as those remaining, will be noted.

As stated in Section B, only an approximate value has been obtained for  $\Delta E$  for room temperature reversibly adsorbed water. This author suggests that such measurement be further refined, and has made preliminary attempts to do so. One possibility is the purchase of an expensive hygrometer. The other approach, tried here, was to work with water vapor alone.

Instead of bubbling  $N_2$  through water, the sample chamber was evacu-

ated (to 50 $\mu$  or lower) and then opened to a vessel containing outgassed, distilled H<sub>2</sub>O. When the vacuum pump was closed off, the pressure could be allowed to rise to various values before shutting off access to the water. Then the measured total pressure would be the pressure of water vapor present.

The first problem was to read pressures in the range from zero to eighteen m.m. (the handbook value of water's vapor pressure at room temperature). On a mercury manometer it would be difficult to read a 10% change here. A Macleod gage compresses the gas, and since this is a vapor, it would condense. The final decision was to use an oil manometer, magnifying the reading by about a factor of thirteen.

The system with an oil manometer was not adequate to cope with excessive vapor condensation on the system walls, subsequent freezing, and the consequent slowing of evacuation due to slow subliming of the ice. This might be overcome by thermostating the system.

A crucial factor in design of a future system is to provide for low pressures held stable for long times by either a very tight vacuum system, or a rearrangement such that dynamic pumping would be possible.

An obvious extension from the present work, which might yield interesting results upon further study, is the adsorbate used. This study confined itself to H<sub>2</sub>O, but many others could be tried. Some work has been done here on the kinetics of O<sub>2</sub> adsorbed on SnO<sub>2</sub>, but none on its flash desorption. One difficulty will be picking a maximum temperature high enough so desorption is essentially complete but low enough so that bulk changes have not begun.

Another point of departure offered is the anomaly seen in Fig. (17). Although not of direct importance to the present work, this behavior may



be interesting on its own. Perhaps a theoretical approach along the lines of Section I-D could show the anomaly to be due to the heating itself. Failing that, it is possible that it could be tackled experimentally.

There is much room left for work concerning the flash desorption model. Eq. (18) should be replaced by a model built up from chemical kinetics expressions like Eq. (8).

#### D. Conclusions

This section is a summary of the conclusions to be drawn from the above work.

The first conclusion is that water ionically adsorbs onto  $\text{SnO}_2$  in two temperature ranges. Desorption in the low range is completed by  $400^\circ\text{K}$  and desorption in the high range begins around  $600^\circ\text{K}$ . The adsorption processes in the two different ranges are probably different in character, but the evidence thus far does not warrant this as an absolute conclusion.

The second conclusion is that at room temperature water can with the aid of a as yet unknown trace element be adsorbed irreversibly; that is, adsorbed in such a way that it desorbs only in the high temperature range. The crucial ambient component is identified as a catalyst (or an aid in some less direct way, e.g. inhibiting a competing process) that disappeared rather than a direct inhibitor that appeared on the strength of the work reported in Section B. The possibility of some non-ambient surface pollutant is ruled out by the same results that served to identify the irreversibly adsorbed water with the high temperature reversibly adsorbed water: the close comparison of ranges of desorption and de-

sorption energies between Fig. (18) and Fig. (21).

The third conclusion is that in both temperature ranges the adsorption kinetics follow the Elovich equations. This is seen in Figs. (12), (13), and (25) through (30).

The fourth conclusion is that in the low temperature range the adsorption has a  $\Delta E$  of about one and a half electron volts, as discussed in connection with Fig. (24).

The fifth conclusion is that in the high temperature range the desorption appears of zeroth order and shows that the two energies seen in Fig. (18) are  $E_d = 1.17$  ev and 0.62 ev.

## BIBLIOGRAPHY

1. Wykoff, R. W. G., Crystal Structures, Interscience Publishers, New York (1963).
2. Baur, V. W. H., *Acta Cryst* 9, 515 (1956).
3. Loch, L. D., *J. Electrochem. Soc.* 110, 1081 (1963).
4. Kohnke, E. E., *J. Phys. Chem. Solids* 23, 1557 (1962).
5. Smitt, R., J. A. Marley, and N. F. Borelli, *J. Phys. Chem. Solids* 25, 1465 (1964).
6. Smitt, R., and N. F. Borelli, *J. Phys. Chem. Solids* 26, 921 (1965).
7. Houston, J. E. and E. E. Kohnke, *J. Appl. Phys.* 36, 3931 (1965).
8. Rutledge, J. L., Ph.D. dissertation, Oklahoma State University (1968).
9. Hauffe, K., *Advances in Catalysis* 7, 213 (1955).
10. Morrison, S. R., *Advances in Catalysis* 7, 259 (1955).
11. Matthews, H. E., Ph.D. dissertation, Oklahoma State University (1968).
12. Blakemore, J. S., Semiconductor Statistics, Pergamon Press, London (1962).
13. Bliel, C. E. and W. A. Albers, *Surface Science* 2, 307 (1964).
14. Morrison, R. S., *J. Catalysis* 20, 110 (1971).
15. Kroger, F. A. and H. J. Vink, *Solid State Phys.* 3, 307 (1956).
16. Low, M. J. D., *Chem. Rev.* 60, 267-312 (1961).
17. Medved, D. E., *J. Phys. Chem. Solids* 20, 255 (1961).
18. Matthews, H. E. and E. E. Kohnke, *J. Phys. Chem. Solids* 29, 653-61 (1968).
19. Roseboom, V. E., M.S. Thesis, Oklahoma State University (1968).
20. Balts, K. W., M.S. Thesis, Oklahoma State University (1970).

21. Hurt, J. E., M.S. Thesis, Oklahoma State University (1963).
22. Redhead, P. A., Vacuum 12, 203 (1962).
23. Carter, G., Vacuum 12, 245 (1962).
24. Carter, G., Vacuum 13, 89 (1963).
25. Garlick, G. F. J. and A. F. Gibson, Proc. Phys. Soc. A60, 574 (1948).
26. Braunlich, P., J. Appl. Phys. 38, 2516 (1967).
27. Saunders, I. J., J. Phys. C. (Solid State Phys.) Ser. 2, vol. 2, 2181 (1969).
28. Chen, R., J. Comp. Phys. 4, 415 (1969).
29. Chen, R. and Winer, S. A. A., J. Appl. Phys. 41, 5227 (1970).
30. Paterson, W. L., J. Comp. Phys. 7, 187 (1971).
31. Shenker, D. and Chen, R., J. Phys. D. Appl. Phys. 4, 287 (1971).
32. Jennings, W., First Course in Numerical Methods, The Macmillan Co., New York (1964).
33. Butler, A. and F. Kur, An Introduction to Numerical Methods, Pitman Pub. Co., New York (1962).

VITA<sup>ed</sup>

James K. Sullivan

Candidate for the Degree of

Doctor of Philosophy

Thesis: ADSORPTION OF WATER ON STANNIC OXIDE

Major Field: Physics

Biographical:

Personal Data: Born in Buffalo, New York, July 7, 1943, the son of Charles and Katherine Sullivan.

Education: Graduated from St. Joseph's Collegiate Institute in Buffalo, New York, in 1961; received a Bachelor of Science degree in Physics from Canisius College in 1965; received a Master of Science degree in Physics from St. Louis University in 1967; completed the requirements for the Doctor of Philosophy degree at Oklahoma State University in May, 1972.